

Application of satellite image time series and texture information in land cover characterization and burned area detection

Jinxu Liu

Department of Geosciences and Geography
Faculty of Science
University of Helsinki
Finland

Academic Dissertation

To be presented, with the permission of the Faculty of Science of the University of Helsinki, for public criticism in the lecture hall 5 of the Main Building on September 28th 2017, at 12 o'clock

Helsinki 2017

Supervisors: Professor Petri Pellikka
Department of Geosciences and Geography
University of Helsinki
Finland

Dr. Janne Heiskanen
Department of Geosciences and Geography
University of Helsinki
Finland

Pre-examiners: Professor Martin Herold
Laboratory of Geo-Information Science and Remote Sensing
Wageningen University
The Netherlands

Professor Chaoyang Wu
Institute of Geographic Sciences and Natural Resources Research
Chinese Academy of Sciences
China

Opponent: Professor Timo Tokola
School of Forest Sciences
University of Eastern Finland
Finland

ISSN-L 1798-7911
ISSN 1798-7911 (print)
ISBN 978-951-51-2931-4 (paperback)
ISBN 978-951-51-2932-1 (PDF)
<http://ethesis.helsinki.fi>

Unigrafia
Helsinki 2017

Abstract

Land cover is critical information to various land management and scientific applications, including biogeochemical and climate modeling. In addition, fire is an essential factor in shaping of vegetation structures, as well as for the functioning of savanna ecosystems. Remote sensing has long been an important and effective means of mapping and monitoring land cover and burned area over large areas in a consistent and robust way. Owing to the free and open Landsat archive and the increasing availability of high spatial resolution imagery, seasonal features from the temporal domain and the use of texture features from the spatial domain create new opportunities for land cover characterization and burned area detection.

This thesis examined the application of satellite image time series and texture information in land cover characterization and burned area detection. First, the utility of seasonal features derived from Landsat time series (LTS) in improving accuracies of land cover classification and attribute prediction in a savanna area in southern Burkina Faso was studied. Then, the temporal profiles from LTS were explored for mapping burned areas over a 16 year period, and MODIS burned area product was used for comparison. Finally, the application of texture features derived from high spatial resolution data in land cover classification and attribute predictions was investigated in a savanna area of Burkina Faso and an urban fringe area in Beijing.

According to the results, firstly, seasonal features from LTS based on all available imagery during one year as input led to a significant increase in land cover classification accuracy in comparison to the dry and wet season single date imagery. The harmonic model used for time series modeling provided a robust method for extracting seasonal features, and the influence of burned pixels on seasonal features could be considered simultaneously. Secondly, the annual burned area mapping based on a harmonic model and breakpoint identification with LTS was capable of detecting small and patchy burn scars with higher accuracy than MODIS burned area product. The approach demonstrated the potential of LTS for improving burned area detection in savannas, and was robust against data gaps caused by clouds and Landsat 7 missing lines. Thirdly, predictive models of tree crown cover (CC) using RapidEye and LTS imagery achieved similar accuracy, indicating the importance of texture and seasonal features from RapidEye and LTS imagery, respectively. Predictions of aboveground carbon and tree species richness, which were strongly correlated with CC, were promising using RapidEye and LTS imagery. Finally, the optimized window size texture classification improved classification accuracy in comparison to the classifications with single window size texture features and multiple window size texture features in an urban fringe area in Beijing, indicating the importance of multiscale texture information.

Keywords: Landsat time series, texture, land cover classification, burned area, savanna, tree crown cover

Acknowledgements

This thesis work was conducted at the Department of Geosciences and Geography, University of Helsinki. I really appreciate the opportunity to study and live in Helsinki. It is a quiet and excellent city, which gives me enough freedom and space to be independent. Now it is time to look back to the old days, reflect on my work, and express my sincere gratitude to the people who have helped me throughout this period.

I would like to express my deepest gratitude to my supervisor Professor Petri Pellikka for accepting me as a doctoral student, and providing the continuous support in research and life. Your guidance, encouragement, and assistance are highly appreciated. Special thanks go to my supervisor Dr. Janne Heiskanen, for the inspiring discussion, persistent encouragement, and insightful feedback. Thank you for always being there when I am stuck with my research. It is your help that keep me on track and motive me further in my research. Your warm encouragement makes me highly motivated and more confident in myself. I am grateful to Dr. Matti Mõttus and Dr. Eduardo Maeda for their helpful and valuable suggestions during my study, and I learn a lot from your attitudes towards research. I want to thank all my co-authors for the constructive comment, great contribution and good cooperation.

I am grateful to the pre-examiners, Professor Martin Herold and Professor Chaoyang Wu, for their time and valuable comment in reviewing my thesis. I would like to thank Professor Timo Tokola for being my opponent. I want to thank my grading committee members, Professor Miska Luoto and senior lecturer Petteri Muukkonen.

I would like to thank all the colleagues Hari, Rami, Vincent, Pekka, Mika, Zou, Binyam, Daniela, Temesgen, Edward, Tino, Andrew, Vuokko, Jesse, Viljami, Elisa, Rocío and Zhipeng in our group. In particular, I am grateful to Hari as my officemate for sharing his wisdom in work and life with me. Your encouragement helps me become more open minded and optimistic in life. I would also like to express my thanks to my Chinese friends for their help and support. I really appreciate the help from administration and IT staff in the department. I also want to thank the support from the Chinese Scholarship Council and travel grant from ATM-DP doctoral school.

Finally, I would like to thank my family members for their unconditional love and endless support.

Publication list

- I. **Liu, J.**, Heiskanen, J., Aynekulu, E., Maeda, E.E., Pellikka, P.K.E. 2016. Land cover characterization in West Sudanian savannas using seasonal features from annual Landsat time series. *Remote Sensing*, 8, 365.
- II. **Liu, J.**, Heiskanen, J., Maeda, E.E., Pellikka, P.K.E. 2017. Burned area detection for West African savannas based on Landsat time series. *International Journal of Applied Earth Observation and Geoinformation*, minor revision.
- III. Heiskanen, J., **Liu, J.**, Valbuena, R., Aynekulu, E., Packalen, P., Pellikka, P. 2017. Remote sensing approach for spatial planning of land management interventions in West African savannas. *Journal of Arid Environments*, 140, 29-41.
- IV. **Liu, J.**, Liu, H., Heiskanen, J., Möttöus, M., Pellikka, P. 2014. Posterior probability-based optimization of texture window size for image classification. *Remote Sensing Letters*, 5, 753-762.

Author's contribution

	I	II	III	IV
Conceive and design study	JL, JH	JL, JH, EM	JH, EA	JL, HL
Field design and collection	JH, EA		JH, EA, PPA	
Data analysis	JL, JH, EM	JL, JH, EM	JH, JL, RV	JL, JH, MM
Manuscript	JL	JL	JH, JL	JL
Comments and revision	JH, EM, EA, PPE	JH, EM, PPE	RV, EA, PPA, PPE	HL, JH, MM, PPE

JL=Jinxiu Liu; JH=Janne Heiskanen; EM=Eduardo Maeda; PPE=Petri Pellikka; MM=Matti Möttöus; HL=Huiping Liu; EA=Ermias Aynekulu; RV=Ruben Valbuena; PPA=Petteri Packalen

Abbreviations

AGC	Aboveground Carbon
AVHRR	Advanced Very High Resolution Radiometer
BAI	Burned Area Index
BAP	best-available-pixel
BFAST Monitor	The Breaks For Additive Season and Trend Monitor
CC	Tree Crown Cover
CDR	Climate Data Record
DBH	Diameter at Breast Height
ECVs	Essential Climate Variables
EROS	Earth Resources Observations and Science
ETM+	Enhanced Thematic Mapper Plus
EVI	Enhanced Vegetation Index
GCOS	Global Climate Observing System
GLCM	Gray level Co-occurrence Matrix
GNDVI	Green NDVI
LDSF	Land Degradation Surveillance Framework
LTS	Landsat Time Series
MODIS	Moderate Resolution Imaging Spectrometer
NDVI	Normalized Difference Vegetation Index
NIR	Near Infrared
OLI	Operational Land Imager
OLS	Ordinary least squares
PCA	Principle Component Analysis
RENDVI	Red Edge NDVI
RF	Random Forest
RMSE	Root Mean Square Error
S	Tree species richness
SOC	Soil Organic Carbon
SPOT	Satellite Pour l'Observation de la Terre
SR	Simple Ratio
SVM	Support Vector Machine
SWIR	Shortwave Infrared
TM	Thematic Mapper
VERI1	Vogelmann Red Edge Index

Contents

- 1 Introduction** 9
 - 1.1 Land cover characterization..... 9
 - 1.2 Objectives of the thesis 11
- 2 Background** 12
 - 2.1 Temporal perspective: Landsat time series 12
 - 2.2 Spatial perspective: texture analysis 13
 - 2.3 Burned area detection 14
- 3 Material and methods** 16
 - 3.1 Study areas 16
 - 3.2 Datasets 18
 - 3.2.1 Satellite imagery 18
 - 3.2.2 Field data 19
 - 3.3 Time series analysis 20
 - 3.3.1 Time series model 20
 - 3.3.2 Breakpoint detection 20
 - 3.3.3 Identifying burned area using Landsat time series 21
 - 3.4 Texture analysis 21
 - 3.5 Classification and regression methods 22
- 4 Results** 22
 - 4.1 Seasonal features for land cover classification in savannas 22
 - 4.2 Burned area detection using burned area index time series 24
 - 4.3 Seasonal and texture features in predictive models 25
 - 4.4 Optimal window size to compute texture features for land cover classification 26
- 5 Discussion** 27
 - 5.1 The potential of seasonal features in land cover characterization 27
 - 5.2 Feasibility of the harmonic time series model for seasonal feature extraction 28
 - 5.3 Factors influencing burned area detection accuracy 28
 - 5.4 Insights on the use of texture features 29
- 6 Conclusions** 31
- References** 33

1 Introduction

1.1 Land cover characterization

Land cover is a fundamental variable that refers to the biophysical attributes of the Earth's surface, such as vegetation cover, water, bare soils, and human infrastructure (Foody 2002; Lambin et al. 2001; Gómez et al. 2016). It is critical information for studies of climate change, carbon cycling, hydrology, biodiversity, and food security; in addition, accurate land cover information is essential for natural resource management and policy making (Bounoua et al. 2002; Jung et al. 2006; Miller et al. 2007; Wulder and Coops 2014; Herold et al. 2016). Land cover is a detectable indicator and a good proxy for understanding the dynamics of the Earth's surface (Herold et al. 2006). Land cover characteristics can provide information on ongoing processes of deforestation, urbanization, and loss of biodiversity (Herold et al. 2008). Therefore, timely and reliable land cover information is critical for many planning and management activities, in addition to scientific applications.

Remote sensing has been an important and effective approach to monitoring land cover, particularly due to its ability to collect data over a large area as compared to field survey (Franklin and Wulder 2002; Joshi et al. 2016). Many land cover maps have been produced using remote sensing data on global and regional scales (Hansen et al. 2000; Loveland et al. 2000; Friedl et al. 2002; Gong et al. 2013). The land cover information derived from remote sensing data can be expressed as discrete classes or continuous land cover attributes (Heiskanen 2006; Colditz et al. 2011; Pengra et al. 2015). Image classification is a popular approach to extracting discrete land cover types from remote sensing images. Many studies have used different approaches to predicting continuous land cover attributes, such as tree crown cover (CC), aboveground carbon (AGC), soil organic carbon (SOC), and tree species richness (S) (Halperin et al. 2016; Eckert 2012; Zhu and Liu 2015; Forkuor et al. 2017; Maeda et al. 2014). The prediction of land cover attributes as continuous variables enables the definition of classification legends more flexible, so that it can better meet the users' needs (Cihlar 2000). Moreover, CC is an essential attribute in forest definition, and is often mapped as a continuous variable by remote sensing (Hansen et al. 2002; Heiskanen and Kivinen 2008). Soil attributes related to agricultural productivity and land degradation are important for land management interventions (Vågen et al. 2013). The assessment of biodiversity can be conducted in many ways, and species richness is one of the most commonly used indices (Rocchini et al. 2015).

Many studies have explored the potential of land cover characterization using coarse resolution satellite Earth observation data, due to its high temporal resolution and large spatial coverage, including Moderate Resolution Imaging Spectrometer (MODIS) data, Advanced Very High Resolution Radiometer (AVHRR) data, and Satellite Pour l'Observation de la Terre (SPOT) data (Hansen et al. 2000; Loveland et al. 2000; Friedl et al. 2002; Friedl et al. 2010). However, land cover characterization on a local scale requires detailed and accurate data for social and management activities. Medium (10-100 m) and high spatial resolution (≤ 10 m) Earth

observation data (i.e. Sentinel, Landsat, RapidEye, SPOT-5) can satisfy the requirements of local studies, and have recently become increasingly popular. In addition to the spectral dimension of the medium and high spatial resolution Earth observation data, the use of temporal and spatial dimensions as supplemental information has been proven beneficial for improving the performance of land cover characterization.

Savanna is an ecosystem which consists of a continuous layer of grass interspersed with scattered trees and shrubs (Cahoon et al. 1992). Savannas account for about 60% of the surface of tropical Africa, and human activities have a large influence on their appearance and degradation status (Callo-Concha et al. 2013). The southern part of Burkina Faso is located in the West Sudanian savanna, where there is a high potential for agriculture due to the fertile soils and abundant rainfall (Knauer et al. 2017). Due to the rapidly growing population in Burkina Faso, there is an increasing demand for land resources, leading to unsustainable land cover changes and loss of biodiversity (Kalema et al. 2015). Accurate monitoring and mapping of land cover and change is important, and needed for environmental management. However, the frequent cloud coverage in this area makes land cover mapping a challenging task.

There are frequent and extensive bush fires in African savannas, accounting for a large proportion of the total global burned area (Dwyer et al. 2000; Archibald et al. 2009; Musyimi et al. 2017). Fires, which occur mostly due to anthropogenic reasons, have both positive and negative effects. Fire is an important positive ecological determinant of the African savanna and grassland vegetation types (Higgins et al. 2000; Siljander 2009). The fires emit large amounts of greenhouse gases and aerosol particles, which influence the carbon cycle and can drastically alter vegetation cover (Nielsen and Rasmussen 1997; Mouillot et al. 2014; Giglio et al. 2010; Schroeder et al. 2008). Frequent burning of the savanna can also lead to land degradation and loss of biodiversity (Laris 2005). Therefore, accurate mapping and monitoring of burned area in savannas is crucial for social and environmental applications (Boschetti et al. 2015).

With the enormous growth in population and economy, land use and land cover changes take place rapidly in urban fringe areas, and lead to a process of urbanization (Xue et al. 2013). The characteristic of the spatial patterns in urbanization is the conversion of rural land into urban land in order to satisfy the increasing demand (Liu and Zhou 2005). An accurate and timely understanding of urban dynamics from remote sensing data is increasingly necessary for urban planning and management. High spatial resolution data are of particular benefit in monitoring urbanization, as they are capable of capturing spatial patterns in detail. However, the spectral variability within a particular class increases, making the classification based on spectral information only even harder (Agüera et al. 2008). The approach of combining both spectral and texture information has been developed and proven effective in improving land cover classification accuracy (Berberoglu et al. 2007).

Previous studies show that the incorporation of temporal information from time series data and texture information from high spatial resolution data improves the accuracy of land cover

characterization, but relatively few studies have been conducted in the savanna area in West Africa. The burned area detection approach using multi-temporal information has been constrained to two date comparisons, and there is potential for time series approaches using the full temporal information contained in the Landsat archive to improve burned area detection performance. Furthermore, the texture features derived from high spatial resolution imagery are widely used in urban studies, but the determination of parameters (i.e. window size, combination of texture measures) in texture features extraction has not yet been comprehensively studied.

1.2 Objectives of the thesis

The main objective of this thesis was to assess the potential of seasonal and textural information from Landsat time series (LTS) and high spatial resolution imagery for land cover classification, land cover attribute prediction, and burned area mapping in two case study areas. The more detailed objectives and contents of the four Papers (I-IV) constituting this thesis are summarized below and in Figure 1.

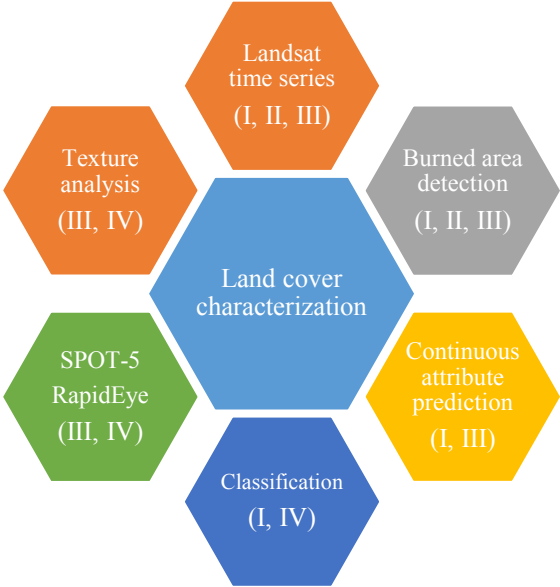


Figure 1. Key words describing the main contents of the thesis and four Papers (I-IV).

Paper I examined the potential of seasonal features to improve the accuracy of land cover classification and CC prediction in a savanna area in southern Burkina Faso. The dry and rainy season single date images were used for comparison to assess the utility of seasonal features. In addition, the effect of burned areas on seasonal features was evaluated. Paper II explored the potential of using LTS for annual burned area mapping in southern Burkina Faso. The burned area detection methodology was developed and applied to 16 years of Landsat data. The results from LTS were also compared with MODIS burned area product. Paper III compared predictive

models for mapping various tree, soil, and species diversity attributes in southern Burkina Faso using spectral, textural, and seasonal features from RapidEye and LTS. Paper IV studied how the window size in texture analysis affects land cover classification accuracy with SPOT-5 image in an urban fringe area of Beijing, and aimed to optimize the texture window size for land cover classification.

2 Background

2.1 Temporal perspective: Landsat time series

The Landsat satellite image archive stores more than four decades of Earth observations, providing an unparalleled record of the status and dynamics of the Earth (Cohen and Goward 2004). Since the beginning of the free and open access policy to the Landsat archive in 2008, Landsat imagery have become a consistent source of medium resolution data for monitoring land cover and change in near-real time over large areas (Woodcock et al. 2008; Wulder et al. 2012). Data from the recently launched Landsat 8 and Sentinel-2 satellites further increases the frequency of geometrically and radiometrically compatible Earth observations. Specifically, LTS brings two key elements to land cover monitoring: a spatial dimension that is ideal and appropriate for regional land cover mapping (Townshend and Justice 1988), and a temporal dimension that enables the monitoring and detecting of land cover with a tremendously rich archive of long term Earth observations (Wulder et al. 2012).

Vegetation seasonality, or phenology, refers to the study of periodic plant life cycle events, and is particularly useful for land cover classification, especially for vegetation cover mapping (Wu et al. 2016). The seasonal information contained in a time series remote sensing data is capable of depicting vegetation growth and the shape of vegetation growing profiles (Brown et al. 2013; Xiao et al. 2002). It has been proven that temporal information from time series remote sensing data is particularly helpful in the identification of land cover types, especially types dominated by vegetation, and has also been successfully applied to the identification of forest disturbances, cloud cover, and urbanization (Jia et al. 2014 ; DeVries et al. 2015; Goodwin et al. 2013; Fu and Weng 2016). For example, phenological differences can increase discrimination between herbaceous crops and savanna vegetation (Senf et al. 2015), or crops and pastures (Müller et al. 2015).

Approaches to time series analysis in remote sensing have long been applied to coarse spatial resolution data, such as pixel-based compositing with AVHRR and MODIS data (Cihlar et al. 1994; Justice et al. 2002). With the advent of free Landsat imagery, an increasing number of observations have been made available to users, and compositing approaches have become more relevant and popular for Landsat applications, including land cover characterization. The best-available-pixel (BAP) composite approach aims to produce large area, cloud free surface reflectance composites by selecting the best available observation matching the user defined criteria (e.g. target day of year, cloud cover, sensor) (White et al. 2014). However, an important

limitation of the BAP approach is missing data, such as pixels with no observations due to clouds, cloud shadows, sensor issues (e.g. Landsat 7 ETM+ SLC-off gaps), or restricted acquisition period. Furthermore, the BAP approach does not make full use of the seasonal information in the time series, as only the single best pixel is selected. Therefore, alternative approaches utilizing all the cloud free observations are needed.

There are several methods to derive seasonal or temporal features from LTS. Pixel-based statistical metrics (e.g. average, maximum, minimum, and variability) derived from multi-temporal spectral data and vegetation indices are commonly used as inputs in land cover classification and continuous attributes prediction (Jia et al. 2014; Potapov et al. 2012; Karlson et al. 2015). Furthermore, a number of temporal trajectory approaches have been developed in recent years. For example, TIMESAT software is a popular tool for seasonal feature extraction (Jönsson and Eklundh 2004). Metrics such as the beginning, end, and length of a growing season derived from vegetation index time series can be used as input data in land cover classification to separate vegetation types with unique phenological characteristics (Brandt et al. 2016).

Also, an approach based on the harmonic model has been increasingly applied in land cover classification, change detection, forest disturbance mapping, cloud detection, and land surface temperature data generation (Zhu and Woodcock 2014a; DeVries et al. 2015; Zhu and Woodcock 2014b; Fu and Weng 2016). The advantage of the method is that it allows the use of all available Landsat imagery with missing values due to clouds and cloud shadows or sensor malfunctioning (e.g. Landsat 7 ETM+ SLC-off gaps). However, because of the lower data availability due to persistent cloud cover in rainy season (Ernst et al. 2013; Mitchard et al. 2011) or excessive gaps in the Landsat archive (Broich et al. 2011), there are relatively few studies demonstrating the seasonal features derived from the harmonic model and LTS for land cover characterization in tropical African savanna.

2.2 Spatial perspective: texture analysis

With the development of remote sensing technology, high spatial resolution satellite imagery have become an essential data source for a wide range of applications, such as land cover classification, forest structure variable prediction, soil mapping, and habitat modeling (Agüera et al. 2008; Kayitakire et al. 2006; St-Louis et al. 2006; Culbert et al. 2012). Conventional approaches which use only spectral information have proved ineffective when applied to land cover classification, due to the complex spectral characteristics of land cover types (Puissant et al. 2005). Many studies have found that texture can play an important role in improving the performance of land cover classification using high spatial resolution imagery (Puissant et al. 2005; Ghimire et al. 2010), but it has also been used earlier with airborne remote sensing imagery (e.g. Pellikka et al. 2000). In studies of continuous land cover attributes prediction, the most widely used predictors are spectral bands and vegetation indices (Sarker and Nichol 2011). Texture features derived from high spatial resolution data have recently been used to aid in

forest structure variables prediction (Pargal et al. 2017). Previous studies report that texture features correlate better with field data measurements, since they allow for the identification of different vegetation structural details, and are capable of enhancing vegetation discrimination (Dube and Mutanga 2015).

Texture refers to the visual effect caused by spatial variation in tonal quantity over relatively small areas (Feng et al. 2015). Texture analysis provides information on the local spatial structure and variability of land cover types in the spatial dimension. Many texture feature extraction methods have been proposed; for example, the gray level co-occurrence matrix (GLCM), Gabor filters, wavelet features, and Markov random fields (Ouma et al. 2006). GLCM (Haralick et al. 1973) is an effective and popular method to extract texture features (Shaban and Dikshit 2001; Pacifici et al. 2009). GLCM features are usually calculated using an odd-sized moving window, and the accuracies of the classification procedure and attributes prediction using texture measures depend largely on the selected window size (Huang et al. 2007; Kayitakire et al. 2006).

A number of studies have been carried out on testing and comparing different window sizes, with the aim of finding an optimal window size (Chen et al. 2004; Puissant et al. 2005; Kayitakire et al. 2006). However, the optimal window size for texture measurements is highly dependent on the image spatial resolution and the land cover characteristics (Pesaresi 2000; Zhu et al. 2012a). Generally, in order to include the entire texture pattern, a large window size should be selected; in contrast, a small window size should be used to include only one land cover type (Dell'Acqua and Gamba 2006; Zhu et al. 2012a). In addition, both the pixel size and the size of the objects of interest should be considered. However, the current methods used for image texture analysis in land cover classification depend on a single moving window, and ignore the various scales of different land cover types in texture features. Furthermore, the feasibility of texture features for predicting continuous land cover attributes in savannas has not yet been fully examined.

2.3 Burned area detection

Fire is recognized as a critical land surface disturbance, causing severe economic, ecological, and atmospheric effects (Vivchar 2011). Burned area is also included in the list of 13 terrestrial essential climate variables (ECVs) by the Global Climate Observing System (GCOS) (Food and Agriculture Organization of the United Nations, 2008). Analyses of past and present burned area patterns can assist in selecting proper fire management practices, and benefit a range of resource management objectives (Dempewolf et al. 2007; Koutsias et al. 2013). Remote sensing is recognized as an essential source of information for mapping burned areas from regional to global scales. Global scale burned area mapping has primarily been derived from coarse spatial resolution data such as MODIS, AVHRR, and SPOT VEGETATION (Siljander 2009; Roy et al. 2008; Giglio et al. 2010; Carmona-Moreno et al. 2005; Tansey et al. 2008). However, burned area products derived from coarse resolution data cannot provide enough spatial detail, and do

not meet the requirements of climate modeling at local and regional scales (Siljander 2009; Roy and Boschetti 2009; Bastarrika et al. 2011). The medium and high spatial resolution satellite images are preferable for accurate monitoring of burned areas at local and regional scales (Chuvieco et al. 2002), and Landsat imagery have been widely used for regional-scale burned area mapping (Miller and Thode 2007; Boer et al. 2008).

The methods for monitoring and mapping burned areas using remote sensing data include: manual digitalization of burned areas (Silva et al. 2005), supervised image classification such as decision trees and neural networks (Kontoes et al. 2009; Maeda et al. 2009), logistic regression (Siljander 2009), principal component analysis (Koutsias et al. 2009), region growing (Hardtke et al. 2015), and threshold-based methods with single date or multi-date images using spectral indices such as the global environmental monitoring index (GEMI), the normalized burned ratio (NBR), and the burned area index (BAI) (Chuvieco et al. 2002; Bastarrika et al. 2011; Musyimi et al. 2017). Burned area detection using multi-temporal information with Landsat imagery has been limited to two date comparisons (Goodwin and Collett 2014).

Due to the diverse and complex patterns of the spectral response of burned areas over space and time, detection and mapping of burned areas using remote sensing image comparisons remains challenging. It can be difficult to acquire and compare cloud free images of pre-fire and post-fire conditions due to the cloud contamination especially in West Africa. The comparison process requires that the two images be obtained within the same season, to minimize the phenology effect. Burned areas demonstrate a wide range of spectral characteristics, caused by the severity of the fire, the vegetation burned, atmospheric conditions, and image acquisition date (Chuvieco et al. 2006; Stroppiana et al. 2012). Moreover, spatially fragmented small patches of burn scars, and the old and new burn scars can be more challenging to detect with remote sensing images (Bastarrika et al. 2014). Although the image comparison approach can provide good results for a particular region, it can be difficult to extend to other locations. Therefore, more robust and automated methods for burned area mapping are needed.

With the release of the Landsat archive freely available to the public, mapping burned areas at Landsat resolution back to the mid-1980s is now possible. There has been considerable research undertaken to characterize trends, and disturbances using temporal information contained in LTS. Kennedy et al. (2007) proposed an automatic trajectory based change detection method using annual LTS for detecting disturbances. Huang et al. (2009) developed a vegetation change tracker algorithm to map forest disturbance. Goodwin et al. (2013) screened clouds and cloud shadows automatically using all available time series of Landsat imagery. However, there are few studies using LTS for monitoring burned area dynamics, and a robust, automatic, and efficient algorithm utilizing LTS for burned area detection is required. Moreover, the effects of burned areas on seasonal features from LTS are not clear, and the pre-processing step of burned area detection before classification study using LTS should be investigated for a better understanding of the possible effects of burn scars on seasonal features. Two Landsat images

in Figure 2 illustrate burn scars in dry season and savanna landscape in wet season in southern Burkina Faso.

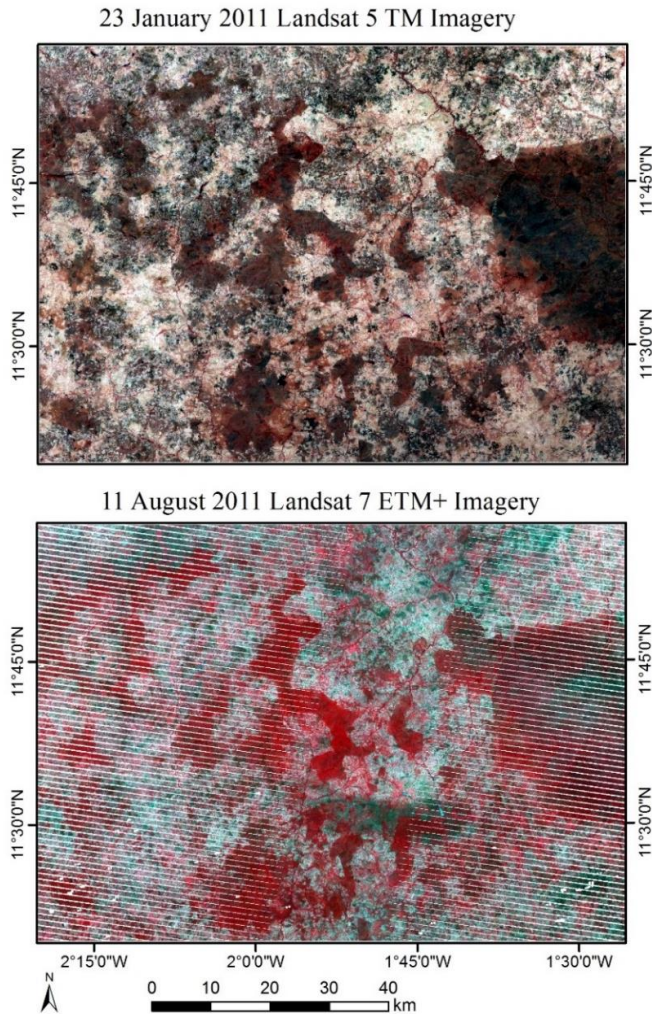


Figure 2. The dark burn scars are clearly visible on dry season Landsat 5 TM image (RGB: NIR, red and green bands) acquired on 23 January 2011. Seasonal variation in reflectance in savanna is large between the dry season image and rainy season Landsat 7 ETM+ image (RGB: NIR, red and green bands) acquired on 11 August 2011.

3 Material and methods

3.1 Study areas

Research was conducted in two study areas: the savanna area in southern Burkina Faso, and an urban fringe area in Beijing (Figure 3, Figure 4). The first study area (Papers I, II, and III) was

located in Ziro and Sissili provinces in southern Burkina Faso in West Africa. The mean annual precipitation is 827 mm, and the mean annual temperature is 27.5 °C for the period 1950–2000 (Hijmans et al. 2005). The topography is relatively flat with a mean elevation of 350 m above sea level. The study area belongs to the West Sudanian savanna ecoregion (Olson et al. 2001), and vegetation consists of tropical dry forests and woodlands surrounded by agroforestry parklands and cultivated lands. The agricultural farming system is a mixture of traditional subsistence farming (i.e. sorghum, millet, maize) and the cultivation of cash crops (i.e. cotton, sesame, peanuts). Forests are partly under community forest management and protection, which provide a sustainable fuelwood production (Coulibaly-Lingani et al. 2011). Southern Burkina Faso has experienced a rapid population growth, which is mostly driven by the immigration of farmers, and has led to land cover changes, particularly the conversion of forest and woodland to cropland (Ouedraogo et al. 2009). Regular fires due to anthropogenic and natural causes are a typical feature of this region (Sawadogo et al. 2002). The majority of the fires take place during the dry season, in November, December, January, and February, extending even into early October, and very late in March and April (Gessner et al., 2015). The fires have not led to permanent land cover changes, and typically the burned vegetation recovers quickly (Silva et al. 2005).



Figure 3. Landscape in savanna area of southern Burkina Faso. (a) Typical savanna woodland close to village of Vrassan. (b) Agricultural landscape with scattered *Vitellaria paradoxa* trees, settlements, and livestock. (Photos: Janne Heiskanen)

The second study area (Paper IV) was an urban fringe area located on the border between Shunyi and Changping districts in Beijing, China (Figure 2). With the development of urbanization and industrialization, this area has experienced rapid land cover change. Based on the characteristics of the land cover types in the study area, five classes were identified, including impervious surfaces, bare land, crops, trees, and water. As there was some spectral confusion between the impervious surfaces and the bare land in the land cover classification, the study area was selected to explore the potential of texture features.

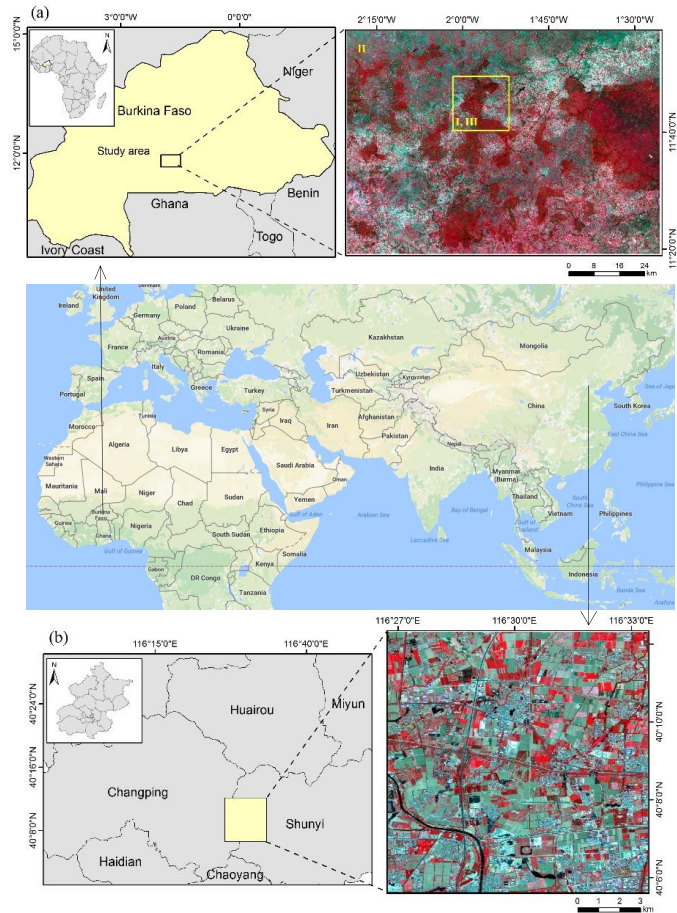


Figure 4. The location of the study areas with false colour satellite image composites: (a) Burkina Faso (Landsat 8 image) with the full study area of Paper II and the subset study area (yellow box) of Papers I and III; (b) Beijing (SPOT-5 image).

3.2 Datasets

3.2.1 Satellite imagery

The satellite imagery and data product used in this thesis are summarized in Table 1. All available Landsat Surface Reflectance Climate Data Record (CDR) data for WRS-2 coordinates Path 195 and Row 52 were downloaded for the period between October 2000 and April 2016 from the USGS Earth Resources Observations and Science (EROS) Center archive. There were in total 281 imagery, including 40 Landsat 5 Thematic Mapper (TM) imagery, 185 Landsat 7 Enhanced Thematic Mapper Plus (ETM+) imagery, and 56 Landsat 8 Operational Land Imager (OLI) imagery. The product has been atmospherically corrected, and clouds and shadows have been detected with Fmask algorithm (Zhu and Woodcock 2012b). Blue, green, red, near-infrared (NIR), and two shortwave infrared (SWIR1, SWIR2) bands were used for further

analysis. In Papers I and III, an annual LTS consisting in total of 35 imagery between November 2013 and October 2014 (14 Landsat 7 ETM+ and 21 Landsat 8 OLI images) were used. In Paper II, the complete time series was used. MODIS burned area product (MCD45A1) between October 2000 and April 2016 was also acquired for comparison in Paper II.

In Paper III, four RapidEye imagery acquired on 4, 7 and 16 February 2014 were used to cover the study area. Imagery included five spectral bands (blue, green, red, red edge, and near infrared) with a spatial resolution of 5 m. The DN values were converted to radiance with radiometric scale factor, and the atmospheric correction was conducted using ENVI FLAASH algorithm (Exelis Visual Information Solutions, Inc.). Due to the reflectance differences between RapidEye imagery, a relative calibration of the spectral bands by linear regression was made based on overlapping areas.

In Paper IV, a SPOT-5 multispectral image acquired on 19 May 2007 was used. The image included green, red, and near infrared bands with 10 m resolution, and shortwave infrared band at 20 m resolution. In order to match other spectral bands with the same spatial resolution, the shortwave infrared band was resampled to 10 m resolution. The pre-processing procedure included geometric correction with 124 ground control points, and the total root mean square error was 0.6 pixels. Atmospheric correction was not performed, as it is not necessary when classifying a single image (Song et al. 2001).

Table 1. Satellite imagery and data products used in the different Papers (I-IV).

Imagery	Period	Number
Landsat ETM+ and OLI (I, III)	November 2013 - October 2014	35
Landsat TM, ETM+ and OLI (II)	October 2000 - April 2016	281
MODIS burned area product (II)	October 2000 - April 2016	187
RapidEye Imagery (III)	4, 7 and 16 February 2014	4
SPOT-5 Imagery (IV)	19 May 2007	1

3.2.2 Field data

Field data was used in Papers I and III as training data for classification, and for building predictive models for vegetation and soil attributes. The field data were collected from 160 sample plots from December 2013 to February 2014. The sampling design followed Land Degradation Surveillance Framework (LDSF) protocol (Vågen et al. 2013). The study area (10 km × 10 km) was stratified into 16 tiles, which were randomly sampled by 100 ha clusters. Each cluster had ten randomly placed circular sample plots with a radius of 17.84 m (0.1 ha), which were further sampled by four subplots having a radius of 5.64 m (0.01 ha). The plots were located with a GPS device. Tree species and diameter at breast height (1.3 m, DBH) were measured for all the trees having DBH > 10 cm. Height and crown diameter were measured for the smallest, largest, and median trees. In subplots, all the stems having a diameter between 4 cm and 10 cm were counted, and height, diameter, and species were recorded for the median tree. For stems that were not measured, a non-linear mixed effect modeling was applied for

predicting height, and linear regression for predicting crown diameter (Valbuena et al. 2016). CC was estimated from the canopy area index (Torello-Raventos et al. 2013). The field plots were classified as closed woodland, woodland savanna, and grassland savanna based on the canopy cover and mean tree height, and the cultivated plots were classified as cropland. The biomass was estimated with allometric model (Chave et al. 2014) and converted to carbon with a carbon fraction. Soil organic carbon content and nitrogen concentrations were analyzed from soil samples. Tree inventory was used for calculating tree species richness and diversity indices.

3.3 Time series analysis

3.3.1 Time series model

A harmonic model (Equation 1) was used to capture seasonality of reflectance and normalized difference vegetation index (NDVI). The following model was fitted for each pixel:

$$\hat{y}_t = a + b \times \sin\left(\frac{2\pi t}{T} + c\right) + e_t \quad (1)$$

where \hat{y}_t is a dependent variable (reflectance, vegetation index) on Julian date t , T is 365 as a frequency, a , b , and c are model parameters in the harmonic model (intercept, amplitude and phase, respectively), and e_t is the residual. Parameter a is an estimate of the mean value of the time series, parameter b captures the inter-annual changes caused by vegetation phenology, and parameter c represents the timing of the phenological events. Since the harmonic model can be simplified as a linear model, an ordinary least squares method (OLS) was used to fit it for each pixel. In Papers I and III, the harmonic model was fitted using annual LTS. In Paper II, the model was fitted using LTS of 16 years.

3.3.2 Breakpoint detection

The Breaks For Additive Season and Trend (BFAST) Monitor algorithm has been proved effective in identifying deforestation from stable trajectories and robust in regions with low availability of clear observations in the time series data (Verbesselt et al. 2012; DeVries et al. 2015). The BFAST Monitor method was applied to detect breakpoint in Paper II. The harmonic model was fitted for each pixel NDVI time series using ordinary least squares (OLS) within a stable history period. Then the breakpoint detection was performed over the monitoring period by comparing the new observations and the model predictions. If the absolute value of the moving sums (MOSUM) of the residuals during the monitoring period was significant, a breakpoint was identified. Each pixel-wise time series had its own stable period after breakpoint detection. The pixels without land cover change were regarded as stable from 2000 to 2016, and the pixels with breakpoints were divided into before and after land cover change periods.

3.3.3 Identifying burned area using Landsat time series

The burned area detection method was utilized in Papers I, II, and III. Because burned pixels had higher burned area index (BAI) values than unburned pixels, it was used for detecting burned pixels from the time series data. Zhu and Woodcock (2014b) applied a similar method to detect clouds and cloud shadows remaining after more simple cloud masking. By comparing the actual Landsat observations and corresponding model predictions, it is possible to identify pixels affected by fire.

Some pixels remained stable for the complete 16 year period (i.e. land cover did not change), and the method can be applied to the whole BAI time series. However, otherwise the method needs to be applied to the period before and after land cover change. First, BAI image stack was created from LTS. Second, the harmonic model was fitted for each pixel using all the BAI observations within the stable period as response variable. Third, a threshold was determined to detect burned pixels by comparing the observed and predicted BAI values. The threshold was defined by checking its influence for accuracy, and computed as a difference of predicted BAI value plus 3 times root mean square error (RMSE) and observed BAI value. If the threshold was less than zero, the pixel was identified as a burned pixel. Furthermore, as not all the burned pixels could be detected once, the method was applied iteratively until no more outliers were detected. The harmonic model was fit using the robust iteratively reweighted least squares method, which is robust to outliers (Zhu and Woodcock 2014a). In order to obtain annual burned area from LTS, the burned area detection results were incorporated from the separate imagery during the fire season. Finally, the annual burned area detection results were compared with MODIS burned area product.

3.4 Texture analysis

The statistical measures of the texture features created from GLCM include the mean, variance, homogeneity, contrast, dissimilarity, entropy, angular second moment, and correlation (Haralick et al. 1973). In order to compute the texture features, principle component analysis (PCA) transformation was applied to RapidEye and SPOT-5 imagery, and texture features were extracted from the first principal component (Berberoglu et al. 2007; Wang and Zhang 2014). The interpixel distance was set to one pixel, and measures were averaged over four orientations at a quantization level of 64. Three window sizes were used for RapidEye imagery in Paper III (3×3 pixels, 5×5 pixels and 7×7 pixels). In Paper IV, window sizes from 3×3 pixels to 15×15 pixels were used to extract the features. In addition, the texture features were extracted using an optimized window size. The optimal window size was defined for each pixel based on the posterior probability images from the single window size texture classification based on support vector machine (SVM) classifier. The largest posterior probability was determined for each pixel, and the corresponding window size was used as the optimized window size for texture extraction for that pixel. The texture features extracted using optimized window size were combined with spectral features for the final land cover classification.

3.5 Classification and regression methods

Random Forest (RF) algorithm is an ensemble of tree based classifiers, and has been increasingly applied in applications related to land cover mapping, landscape ecology and attribute prediction (Zhu et al. 2012a; Belgiu and Drăguț 2016). In RF, a large number of classification trees are constructed with bootstrap samples with replacement from the original training data. Each tree is trained using about two thirds of the samples randomly, and the remaining one third of the samples, called out of bag samples, are served to calculate the accuracy. For classification, the output is determined by the maximum number of votes from the group of classification trees. For regression, the prediction is an average of the values from all the trees. There are only two parameters to be optimized: the number of trees and the number of variables to split the nodes.

Here, 500 trees were selected, and the number of variables to split each node was set to the square root of the total number of input variables. In addition, the Random Forest algorithm also provides the variable importance for all the input variables (Breiman 2001). Variable importance is estimated by the difference of the accuracy between the permuted and original out of bag samples. In order to improve the accuracy, in Papers I and III the “VSURF” package in R was adopted to eliminate the least important variables (Genuer et al. 2015). Furthermore, a leave-one-out cross validation method (Brovelli et al. 2008) was performed to evaluate the accuracy.

The SVM classifier has been a widely used method in land cover classification (Pal and Mather 2005), and was used for performing classifications in Paper IV. The advantage of the SVM classifier is that it requires no assumptions about the data distribution, and only a small training sample (Mountrakis et al. 2011; Foody and Mathur 2004). The classification was performed in ENVI 4.5 with default parameters for radial basis function (RBF) kernel. Besides the hard classification output, the posterior probability imagery for each class were also obtained. The incorporation of posterior probability has shown potential for improving land cover classification and change detection (Ibrahim et al. 2005; Gonçalves et al. 2009; Chen et al. 2011). Here, the posterior probability was utilized to help select the window size for each pixel. The training samples were selected with the help of ground knowledge, visual interpretation, and high resolution imagery from Google Earth (Google Inc.) for the period from 25 April 2007 to 10 June 2007. The validation samples were 600 points that were generated according to the stratified random sampling method. McNemar’s test was used to evaluate the significant difference between different classification results.

4 Results

4.1 Seasonal features for land cover classification in savannas

In order to evaluate the effect of burned pixels on seasonal features (time series model parameters), we compared the seasonal features with and without burned pixel removal (Figure

5). The burned pixel removal procedure affected parameter a , representing the mean reflectance of the annual time series only slightly. However, parameter b , which corresponds to the amplitude of reflectance, was affected in NIR band, leading to an increasing variation between different land cover types after burned pixel removal. Cropland differed from other land cover types before burned pixel removal in terms of parameter c , which represents the phase of the reflectance, but all the land cover types had similar parameter c after burned pixel removal.

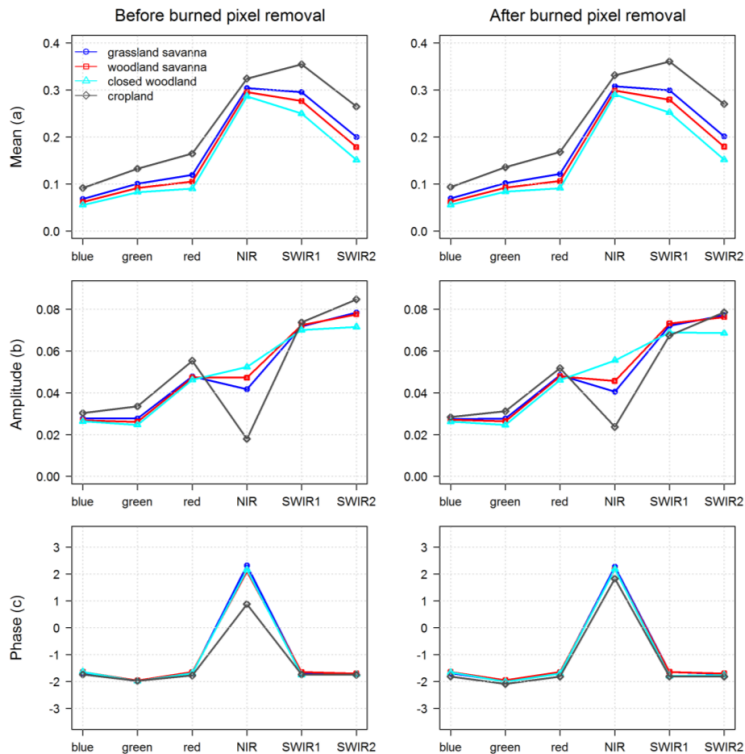


Figure 5. Mean values of seasonal features (time series model parameters) before and after burned pixel removal.

The seasonal features derived from the harmonic model after burned pixel removal clearly increased the overall accuracy from 68.7% and 66.1% to 75.5% in comparison to the dry (12 Nov 2013) and rainy (8 Jun 2014) season single date imagery, respectively, followed by the seasonal features without burnt pixel removal (73.7%). The overall accuracy was further improved by variable selection (76.2%). The selected inputs included parameter a (*mean*) in blue, green, red, SWIR1 and SWIR2 bands, and parameter b (*amplitude*) in NIR band. According to variable importance, parameter a (*mean*) in green, blue, red, SWIR1 and SWIR2 bands, and parameter b (*amplitude*) in NIR band were the most important variables in the seasonal features classification procedure. According to the McNemar's test, the classifications based on seasonal features (both before and after burnt area removal), and the classifications based on the single date images (both dry and rainy season image), were significantly different

($p < 0.05$). Therefore, the results indicate that the seasonal features extracted from LTS can significantly improve land cover classification accuracy in comparison to the single date images.

4.2 Burned area detection using burned area index time series

The burned area detection procedure is demonstrated in Figure 4. The detection procedure was based on the phenomenon that the burned pixels had higher BAI values when compared to unburned pixels, and were outliers in the harmonic model. The detection process was applied iteratively until there were no outliers. In Figure 4, the stable pixel BAI time series was fit with a harmonic model, and the burned pixels were detected iteratively. The detected pixels occurred during the fire season, and were correctly identified as burned pixels based on visual analysis. For BAI time series with breakpoint (Figure 6c and 6d), the breakpoint was identified using the BFAST Monitor method, which then divided the time series into two periods. The harmonic models were fit separately for the two periods, and all the outliers were detected and removed. The detected pixels were then checked, and it was found that the outliers before the breakpoint were all correctly identified as burned pixels, and occurred during the fire season. However, the outliers detected in the period after the breakpoint occurred in July and October, which are not in the fire season, so they were not regarded as burned pixels.

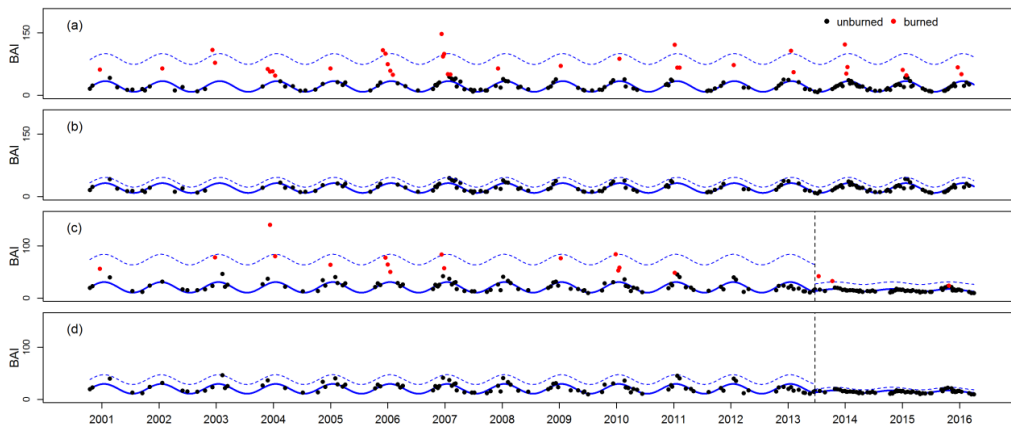


Figure 6. Demonstration of burned area detection for a single pixel without breakpoint (a, b) and with breakpoint (c, d). The black points are the BAI values, the red points are outliers, the blue curve is the harmonic model, and the dashed blue line is the threshold for detecting outliers.

The overall accuracy of burned area detection from LTS was 79.2%, which was higher than that of MODIS burned area product (65.9%). The omission error for Landsat burn scars was 26.9%, much lower than 62.3% for MODIS burned area product, implying that MODIS product omitted more burned areas. The commission errors for LTS and MODIS burned area product were similar, 18.8% and 20.3%, respectively. Specifically, the overall accuracies of Landsat burned area and MODIS burned area product were compared for each year. In general, Landsat fire scars had consistently higher overall accuracies than MODIS burned area product. The

overall accuracy ranged from 70.0% to 91.4% for Landsat fire scars, and from 57.1% and 77.1% for MODIS burned area product. The best overall accuracy occurred during 2014–2015 for both Landsat burn scar and MODIS burned area product.

The proportion of burned area was also computed for 5×5 km grid cells. The comparison of burned areas with Landsat and MODIS at 5×5 km resolution indicated that MODIS burned area product underestimated the amount of burn scars compared to Landsat. Specifically, it was observed that the burned proportion values ranging from 0.1 to 0.3 had a higher frequency in the Landsat results, while the corresponding areas had values close to zero in the MODIS burned area product (Fig. 10 in Paper II). In general, the MODIS burned area showed poor agreement with burn scars detected from Landsat ($R^2 = 0.30$).

4.3 Seasonal and texture features in predictive models

The performances of CC, AGC and S predictions are shown in Table 2. The predictions for CC from RapidEye and LTS imagery achieved similar results, with R^2 of 0.68 and 0.67 respectively. Considering predictions of S, the R^2 was 0.62 for RapideEye imagery and 0.61 for LTS, and the RMSE was the same for RapidEye and LTS imagery. RapidEye imagery provided R^2 of 0.61 and RMSE of 4.2% for AGC prediction, however LTS only achieved R^2 of 0.53 and RMSE of 4.6%. In general, the higher resolution RapidEye imagery provided the best accuracy, but the improvement compared to Landsat imagery was quite marginal. Other response variables (i.e. SOC) which were weakly correlated with CC were poorly predicted (Fig.3 in Paper III).

Table 2. Accuracy of tree crown cover (CC), aboveground carbon (AGC), and tree species richness (S) predictions from RapidEye and LTS imagery.

Response Variable	Input Data	R^2	RMSE	Selected variables ¹
CC	RapidEye	0.68	10.2	blue, green, GNDVI, RENDVI, red, red.sd, RENDVI.sd, contrast, NDVI.sd, entropy
	LTS	0.67	10.4	GNDVI, SR, green.a, blue.a, EVI, SWIR2.a, SWIR1.c
AGC	RapidEye	0.61	4.2	blue, green, VREI1, angular second moment, entropy, red.sd
	LTS	0.53	4.6	SWIR2.a, SR, GNDVI, blue.a, green.a, SWIR1.c
S	RapidEye	0.62	2.4	blue, green, RENDVI, VREI1, red
	LTS	0.61	2.4	GNDVI, blue.a, SR

¹ “blue”, “green”, “red”, “NIR”, “SWIR1”, and “SWIR2” refer to reflectance corresponding to blue, green, red, near-infrared, and shortwave infrared wavelength regions, and suffixes “.a”, “.c”, and “.sd” refer to seasonal parameters *a* (mean), *c* (phase) and standard deviation, respectively.

The variable selection procedure improved model performance, because it eliminated less important predictors among many input variables. Texture features (i.e. contrast, entropy,

angular second moment) were selected when predicting CC and AGC with RapidEye imagery. Other important input variables included reflectance in blue, green bands, vegetation indices such as green NDVI (GNDVI), red edge NDVI (RENDVI), vogelmann red edge index (VERI1) and enhanced vegetation index (EVI) from RapidEye imagery for CC, AGC, and S predictions. For prediction models with LTS, the most important and frequently selected variables included seasonal feature parameter *a* (*mean*) for blue band, GNDVI, and simple ratio (SR). In addition, parameter *a* (*mean*) for green band, parameter *a* (*mean*) for SWIR2 band, and parameter *c* (*phase*) for SWIR1 band were also commonly selected input variables.

4.4 Optimal window size to compute texture features for land cover classification

The texture features improved the classification accuracy in Paper IV in comparison with the classification based on spectral features only. The window size influenced the classification accuracy, and the best overall accuracy was achieved with window size of 7×7 pixels. However, not all the land cover types achieved the best overall accuracy with window size of 7×7 pixels, revealing that there was not a single optimal window size for all the land cover types.

The multiple window size texture classification outperformed the best single window size texture classification. However, the optimized window size texture classification method achieved the best accuracy among all the classifications. The McNemar’s test showed that the best single window size and optimized window size texture classifications were significantly different ($p < 0.05$).

It was also observed that different land cover types had a different distribution of the optimized window size (Figure 7). The smallest window (3×3 pixels) distributed with a high proportion among impervious surface, tree, and water pixels, and these land cover types usually formed irregular shapes in relatively small patches. On the other hand, the largest window of 15×15 pixels was selected by crop and bare land pixels, and these two land cover types usually occurred in large patches with regular rectangular shapes.

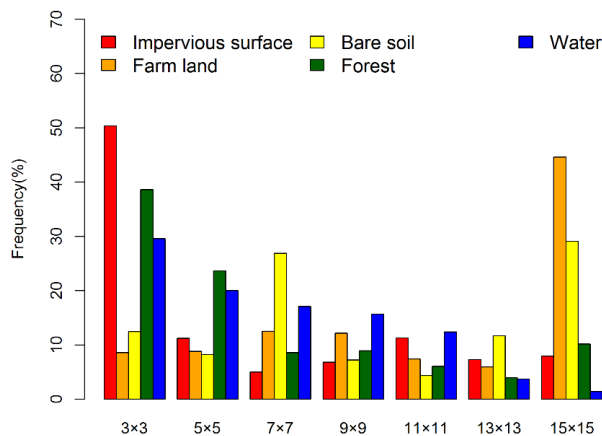


Figure 7. Optimized texture window size distribution for different land cover types.

5 Discussion

5.1 The potential of seasonal features in land cover characterization

The results of Papers I and III indicate that seasonal features from LTS are useful information for land cover characterization, including classification and tree and species diversity attributes prediction, which is consistent with a number of studies from different parts of the world (Heiskanen and Kivinen 2008; Esch et al. 2014; Brandt et al. 2016). In comparison to the single date images, the land cover classification, predictions of CC, AGC, and S using seasonal features from LTS achieved better accuracies. The results are in agreement with Karlson et al. (2015), who found higher accuracies of canopy cover and biomass predictions in Burkina Faso were achieved using statistical seasonal features from dry season NDVI images. This could be explained by the fact that different land cover types exhibit distinctive phenological characteristics and temporal profiles in LTS (Brown et al. 2013). The prediction performances for tree and species diversity attributes demonstrated that the seasonal features from free of cost LTS can be an optional data choice in comparison to high resolution RapidEye data. The seasonal component, representing intra-annual change in LTS, offers new opportunities for land cover characterization in terms of temporal information.

The traditional method of burned area detection depends on bi-temporal image comparison. The method in Paper II provides new insights into depicting spatial-temporal patterns of burned areas and detecting annual burned areas using LTS in savanna areas. The results of Paper II demonstrate that this method is capable of identifying small and fragmented burn scars in comparison to lower resolution MODIS burned area product. The accuracies of classification and CC prediction after burned area removal were better than those without burned area removal, indicating that the burned area affects the seasonal features and harmonic time series model. In particular, it was observed that the reflectance in NIR and SWIR1 bands decreased when compared to pre-fire conditions, because fire destructs the leaf structure of the vegetation (Koutsias and Pleniou 2015). Therefore, the burned area should be considered when seasonal parameters are extracted from LTS data.

As LTS are based on free and open data, and data processing can be automated, it is obvious that the seasonal component in LTS should be considered when conducting land cover classification and tree, soil, and biodiversity attributes prediction. The performance differences between rainy and dry season images for land cover characterization indicate that image selection is required and needed when using single date image. The late dry season imagery performs better than imagery from the rainy season in Papers I and III, which is in line with a previous study that reported imagery from the peak season was less accurate for predicting AGB (Zhu and Liu 2015). The reason for this is that in the rainy season all vegetation types, such as trees, grasses, and crops are green, which decrease their spectral differences. However, due to the phenological differences, imagery from the late dry season provides a better contrast

for different vegetation types (Karlson et al. 2015), and the utilization of LTS can avoid the problem of image selection (Liu et al. 2015).

5.2 Feasibility of the harmonic time series model for seasonal feature extraction

By using all available Landsat imagery, the harmonic time series model enables to construct a current or even historical temporal profile of the Earth's surface. The estimated time series coefficients can be utilized for land cover classification and attributes prediction, which indicate the robustness of the method (Jakubauskas et al. 2002; Zhu and Woodcock 2014a). Furthermore, the harmonic time series model has been successfully employed in forest disturbance studies by comparing the deviation of new observations from the predicted model values (Zhu et al. 2012c; DeVries et al. 2015).

The harmonic time series model has many advantages. It is easily automated, and also capable of monitoring land cover change. In addition, there are no empirical thresholds in studies of land cover change and burned area detection. The thresholds depend on the model estimations and original observations, which are done for each individual pixel separately. Furthermore, the method exploits all available Landsat observations regardless of partially cloudy imagery. Future studies can employ even greater amounts of Earth observations by combining data from Landsat 8 and Sentinel-2, which leads to land cover monitoring in near real-time at medium resolution scale (Wulder et al. 2015). LTS can overcome limitations such as missing lines or gap filling due to clouds and cloud shadows, as only good-quality observations are used for constructing the model. Subjective image selection and mosaicking are not required in a harmonic time series model. When comparing the harmonic model with the BAP compositing method, it does not require the target day for compositing. The statistical metrics (e.g. maximum, minimum, mean of reflectance), which are commonly extracted from cloud-free images to represent seasonal features, depend on the distribution of clear observations over the observation period, but the harmonic time series model does not have this problem.

There are also limitations to the harmonic time series model. It is not applicable in places with persistent cloud or snow cover, as there may be too few clear observations for reliable model fitting. The simple harmonic model could capture the seasonality of different land cover types in the study area in southern Burkina Faso, but a more complicated model might be needed for land cover types with more complicated intra-annual variations.

5.3 Factors influencing burned area detection accuracy

The comparison of the Landsat burned area and MODIS burned area product revealed differences in the burn scar distinction due to image spatial resolution. Landsat was able to capture small and fragmented burn scars, but MODIS burned area product could not capture the same level of spatial detail when burn scars were small. This caused an underestimation of burn scar area by MODIS. These results are consistent with previous studies (Laris 2005; Silva

et al. 2005; Roy and Boschetti 2009), demonstrating the importance of higher spatial resolution data in burned area detection.

The fire season in the study area lasts from November to February, and the vegetation recovers rapidly after a fire event, which makes the spectral distinction unclear and the detection more challenging (Roy et al. 2008). As the low severity fires only show minimal spectral differences when compared to unburned pixels, the burn scars cannot be detected, which leads to omission errors (Hardtke et al. 2015). These errors are emphasized with lower temporal resolution, as burn scars do not occur at the overpass time of the satellite, when they could be easily and best detected (Giglio 2007). Our findings are consistent with earlier studies which also report data gaps due to temporal resolution, and further limitations due to cloud and cloud shadow obstruction (Koutsias et al. 2013; Goodwin and Collett 2014; Boschetti et al. 2015). The use of LTS to characterize temporal profiles in BAI time series facilitated the automation of burned area detection in the algorithm of this thesis, and it would be possible to combine observations from Sentinel-2 with Landsat observations to generate denser time series in future work. However, one disadvantage of the algorithm is the lack of accurate burning date. The relatively low temporal resolution of Landsat imagery is the main reason for this shortcoming.

Discriminating burned area is a significant challenge in applying a time series analysis algorithm across a range of land cover types. Overestimation of burned areas is caused by unmasked cloud shadows, due to the similar BAI values in the temporal profile. Furthermore, errors also arise from cropland and forest, as they are spectrally similar to burned areas in the study area. These results are in agreement with previous studies that reported crop harvesting, rapid vegetation senescence, agricultural areas, and dark soils leading to commission errors due to spectral confusion with burned pixels (Stroppiana et al. 2012; Boschetti et al. 2015). This highlights that a multi-criteria or multi-index approach would be another choice to improve burned area detection accuracy (Bastarrika et al. 2011). In this study, a distinct fire season was defined, which helped to exclude false detections during the wet season. Including land cover types as a criteria could have been another way to increase detection accuracy, because grassland and woodland are frequently burned, whereas agricultural lands are seldom burned in the study area (Devineau et al. 2010; Gessner et al. 2015). The errors from the disturbance detection using the BFAST Monitor algorithm could also result in constructing inaccurate harmonic models for BAI time series, which would further influence the burned area detection accuracy.

5.4 Insights on the use of texture features

The approaches incorporating texture features from high spatial resolution imagery were developed and adopted in land cover characterization in Papers III and IV. Texture features derived from RapidEye and SPOT-5 imagery were selected as important inputs contributing to continuous land cover attribute predictions and land cover classification, and the results agreed

with previous research suggesting that texture features are useful in improving land cover characterization accuracies (Feng et al. 2015; Halperin et al. 2016).

The improvement of AGC prediction from RapidEye imagery shown in Paper III demonstrates the potential of texture features, as texture features are more effective in defining forest structure with fine spatial resolution imagery, especially in heterogeneous regions (Sarker and Nichol 2011). Among the four important selected predictors for AGC prediction using RapidEye imagery, three of them were texture features. These results are in line with the findings that texture features correlate to a greater degree with aboveground biomass and carbon than spectral bands (Kelsey and Neff 2014). Another reason is that spectral indices often saturate in high biomass conditions, but texture features are less sensitive to this problem (Eckert 2012). The CC predictions from RapidEye and LTS obtained promising and similar accuracies, demonstrating the utility of texture and seasonal features in CC estimation in savanna areas. This finding is consistent with that reached by Karlson et al. (2015), who found texture and seasonal features to be important variables when predicting CC. However, accessibility to RapidEye imagery may be restricted due to high costs, and LTS is a freely available alternative data source for predicting CC with similar accuracy. Moreover, the results also indicate that reasonably accurate S predictions can be derived using RapidEye imagery and LTS. However, texture features were not selected as important variables for predicting S, although texture is often assumed to be an essential input in biodiversity studies (Oldeland et al. 2010; Maeda et al. 2014).

Paper IV demonstrated that the incorporation of optimized window size texture features improved classification accuracy significantly, as texture features could decrease classification errors caused by similar spectral reflectance between different land cover types, such as bare land and impervious surfaces in our study area. The traditional method for determining the optimal texture window size is comparing the overall classification accuracies using several window sizes (Chen et al. 2004; Puissant et al. 2005). In addition, the optimal window size for texture features also depends on the spatial resolution of imagery and land cover characteristics (Pesaresi 2000). It has been suggested that window size should be small enough to preserve detailed structures and avoid including several land cover types (Acharyya et al. 2003); by contrast, a large window size was also found to be effective in regions with a homogeneous character (Myint et al. 2004). Therefore, texture features based on single window size cannot be optimal for different land cover types. The multiple window size texture classification and optimized window size texture classification approaches outperformed single window size texture classification, indicating the importance of multi-scale texture features.

From the distribution of posterior probabilities and optimized texture window size distribution images, we found that a larger window size was preferable for cropland and bare land; by contrast, a small window size was preferable for impervious surface and trees. This finding is in line with previous studies, which revealed that the optimal window size for texture features

varies between different land cover types, and the optimal texture window size is highly dependent on the homogeneity or heterogeneity of land cover types (Huang et al. 2007).

6 Conclusions

This thesis examined the application of satellite image time series and texture information to land cover characterization and burned area detection. More specifically, the focus was on investigating the feasibility of utilizing seasonal features based on satellite image time series, exploring the potential of time series data in burned area detection, and assessing the use of texture features in improving land cover classification accuracy and land cover attributes prediction. The study areas were located in the savanna area of southern Burkina Faso in West Africa, and in an urban fringe area in Beijing. The main conclusions of the thesis are presented below.

(1) The use of seasonal features based on harmonic model and LTS show potential for improving the accuracy of land cover classification in savanna area in southern Burkina Faso. Due to the clouds in the wet season and burned areas in the dry season, good quality Landsat imagery without clouds and burned areas are hard to acquire, and the applied method enabled annual land cover characterization using LTS. In addition, as the burned areas influenced the seasonal features based on LTS, this effect should be considered in time series processing and seasonal feature extraction. Considering the robustness of the harmonic analysis method, a data fusion of Landsat and Sentinel-2 images should be considered in future studies. The acquisition dates of Landsat images affect prediction accuracy, and the peak of the growing season is not the optimal time for land cover mapping in savanna areas.

(2) The LTS based on harmonic model and breakpoint identification provides a novel method for annual burned area mapping. The annual burned area from LTS can capture small patchy burn scars and achieve higher accuracy in comparison to MODIS burned area product. It is robust against decreased data availability due to clouds and missing lines, and explores the temporal domain of all available LTS. The method should be evaluated in other landscapes and over larger geographical areas in future studies.

(3) The results show that CC is best predicted using RapidEye and LTS imagery. Attributes such as AGC and S could be predicted most accurately, as they had a strong correlation with CC. The vegetation indices, texture features from high spatial resolution image and seasonal features from LTS, are useful predictors, and the selected important predictors have variations according to different response variables. The predictions from RapidEye imagery showed only marginal improvement in comparison to that from the free of cost LTS.

(4) The optimized window size texture classification can improve classification accuracy in comparison to the classifications with three other input features (i.e. spectral features, spectral and single window size texture features, spectral and multiple window size texture features).

The multiscale texture information is useful in land cover characterization, and posterior probability information helps to obtain the optimal window size for each pixel.

References

- Acharyya, M., De, R. K., & Kundu, M. K. (2003). Segmentation of remotely sensed images using wavelet features and their evaluation in soft computing framework. *IEEE Transactions on Geoscience and Remote Sensing*, *41*, 2900-2905.
- Agüera, F., Aguilar, F. J., & Aguilar, M. A. (2008). Using texture analysis to improve per-pixel classification of very high resolution images for mapping plastic greenhouses. *ISPRS Journal of Photogrammetry and Remote Sensing*, *63*, 635-646.
- Archibald, S., Roy, D. P., WILGEN, V., Brian, W., & SCHOLLES, R. J. (2009). What limits fire? An examination of drivers of burnt area in Southern Africa. *Global Change Biology*, *15*, 613-630.
- Bastarrika, A., Alvarado, M., Artano, K., Martinez, M. P., Mesanza, A., Torre, L., Ramo, R., & Chuvieco, E. (2014). BAMS: A tool for supervised burned area mapping using Landsat data. *Remote Sensing*, *6*, 12360-12380.
- Bastarrika, A., Chuvieco, E., & Martín, M. P. (2011). Mapping burned areas from Landsat TM/ETM+ data with a two-phase algorithm: Balancing omission and commission errors. *Remote Sensing of Environment*, *115*, 1003-1012.
- Belgiu, M., & Drăguț, L. (2016). Random forest in remote sensing: A review of applications and future directions. *ISPRS Journal of Photogrammetry and Remote Sensing*, *114*, 24-31.
- Berberoglu, S., Curran, P. J., Lloyd, C. D., & Atkinson, P. M. (2007). Texture classification of Mediterranean land cover. *International Journal of Applied Earth Observation and Geoinformation*, *9*, 322-334.
- Boer, M. M., Macfarlane, C., Norris, J., Sadler, R. J., Wallace, J., & Grierson, P. F. (2008). Mapping burned areas and burn severity patterns in SW Australian eucalypt forest using remotely-sensed changes in leaf area index. *Remote Sensing of Environment*, *112*, 4358-4369.
- Boschetti, L., Roy, D. P., Justice, C. O., & Humber, M. L. (2015). MODIS–Landsat fusion for large area 30m burned area mapping. *Remote Sensing of Environment*, *161*, 27-42.
- Bounoua, L., DeFries, R., Collatz, G. J., Sellers, P., & Khan, H. (2002). Effects of land cover conversion on surface climate. *Climatic Change*, *52*, 29-64.
- Brandt, M., Hiernaux, P., Tagesson, T., Verger, A., Rasmussen, K., Diouf, A. A., Mbow, C., Mougin, E., & Fensholt, R. (2016). Woody plant cover estimation in drylands from Earth Observation based seasonal metrics. *Remote Sensing of Environment*, *172*, 28-38.
- Breiman, L. (2001). Random forests. *Machine learning*, *45*, 5-32.
- Broich, M., Hansen, M. C., Potapov, P., Adusei, B., Lindquist, E., & Stehman, S. V. (2011). Time-series analysis of multi-resolution optical imagery for quantifying forest cover loss in Sumatra and Kalimantan, Indonesia. *International Journal of Applied Earth Observation and Geoinformation*, *13*, 277-291.

- Brovelli, M. A., Crespi, M., Fratarcangeli, F., Giannone, F., & Realini, E. (2008). Accuracy assessment of high resolution satellite imagery orientation by leave-one-out method. *ISPRS Journal of Photogrammetry and Remote Sensing*, *63*, 427-440.
- Brown, J. C., Kastens, J. H., Coutinho, A. C., de Castro Victoria, D., & Bishop, C. R. (2013). Classifying multiyear agricultural land use data from Mato Grosso using time-series MODIS vegetation index data. *Remote Sensing of Environment*, *130*, 39-50.
- Cahoon, D. R., Stocks, B. J., Levine, J. S., Cofer, W. R., & O'Neill, K. P. (1992). Seasonal distribution of African savanna fires. *Nature*, *359*, 812-815.
- Callo-Concha, D., Gaiser, T., Webber, H., Tischbein, B., Muuml, M., & Ewert, F. (2013). Farming in the West African Sudan Savanna: insights in the context of climate change. *African Journal of Agricultural Research*, *8*, 4693-4705.
- Carmona-Moreno, C., Belward, A., Malingreau, J. P., Hartley, A., Garcia-Alegre, M., Antonovskiy, M., Buchshtaber, V., & Pivovarov, V. (2005). Characterizing interannual variations in global fire calendar using data from Earth observing satellites. *Global Change Biology*, *11*, 1537-1555.
- Chave, J., Réjou-Méchain, M., Búrquez, A., Chidumayo, E., Colgan, M. S., Delitti, W. B., et al. (2014). Improved allometric models to estimate the aboveground biomass of tropical trees. *Global Change Biology*, *20*, 3177-3190.
- Chen, J., Chen, X., Cui, X., & Chen, J. (2011). Change vector analysis in posterior probability space: A new method for land cover change detection. *IEEE Geoscience and Remote Sensing Letters*, *8*, 317-321.
- Chen, D., Stow, D. A., & Gong, P. (2004). Examining the effect of spatial resolution and texture window size on classification accuracy: an urban environment case. *International Journal of Remote Sensing*, *25*, 2177-2192.
- Chuvieco, E., Martin, M. P., & Palacios, A. (2002). Assessment of different spectral indices in the red-near-infrared spectral domain for burned land discrimination. *International Journal of Remote Sensing*, *23*, 5103-5110.
- Chuvieco, E., Riaño, D., Danson, F. M., & Martin, P. (2006). Use of a radiative transfer model to simulate the postfire spectral response to burn severity. *Journal of Geophysical Research*, *111*, G04S09.
- Cihlar, J. (2000). Land cover mapping of large areas from satellites: status and research priorities. *International Journal of Remote Sensing*, *21*, 1093-1114.
- Cihlar, J., Manak, D., & D'Iorio, M. (1994). Evaluation of compositing algorithms for AVHRR data over land. *IEEE Transactions on Geoscience and Remote Sensing*, *32*, 427-437.
- Cohen, W. B., & Goward, S. N. (2004). Landsat's role in ecological applications of remote sensing. *Bioscience*, *54*, 535-545.
- Colditz, R. R., Schmidt, M., Conrad, C., Hansen, M. C., & Dech, S. (2011). Land cover classification with coarse spatial resolution data to derive continuous and discrete maps for complex regions. *Remote Sensing of Environment*, *115*, 3264-3275.

- Coulibaly-Lingani, P., Savadogo, P., Tigabu, M., & Oden, P. C. (2011). Factors influencing people's participation in the forest management program in Burkina Faso, West Africa. *Forest Policy and Economics*, *13*, 292-302.
- Culbert, P. D., Radeloff, V. C., St-Louis, V., Flather, C. H., Rittenhouse, C. D., Albright, T. P., & Pidgeon, A. M. (2012). Modeling broad-scale patterns of avian species richness across the Midwestern United States with measures of satellite image texture. *Remote Sensing of Environment*, *118*, 140-150.
- Dell'Acqua, F., & Gamba, P. (2006). Discriminating urban environments using multiscale texture and multiple SAR images. *International Journal of Remote Sensing*, *27*, 3797-3812.
- Dempewolf, J., Trigg, S., DeFries, R. S., & Eby, S. (2007). Burned-area mapping of the Serengeti–Mara region using MODIS reflectance data. *IEEE Geoscience and Remote Sensing Letters*, *4*, 312-316.
- Devineau, J. L., Fournier, A., & Nignan, S. (2010). Savanna fire regimes assessment with MODIS fire data: their relationship to land cover and plant species distribution in western Burkina Faso (West Africa). *Journal of Arid Environments*, *74*, 1092-1101.
- DeVries, B., Verbesselt, J., Kooistra, L., & Herold, M. (2015). Robust monitoring of small-scale forest disturbances in a tropical montane forest using Landsat time series. *Remote Sensing of Environment*, *161*, 107-121.
- Dube, T., & Mutanga, O. (2015). Investigating the robustness of the new Landsat-8 Operational Land Imager derived texture metrics in estimating plantation forest aboveground biomass in resource constrained areas. *ISPRS Journal of Photogrammetry and Remote Sensing*, *108*, 12-32.
- Dwyer, E., Pinnock, S., Grégoire, J. M., & Pereira, J. M. C. (2000). Global spatial and temporal distribution of vegetation fire as determined from satellite observations. *International Journal of Remote Sensing*, *21*, 1289-1302.
- Eckert, S. (2012). Improved forest biomass and carbon estimations using texture measures from WorldView-2 satellite data. *Remote Sensing*, *4*, 810-829.
- Ernst, C., Mayaux, P., Verhegghen, A., Bodart, C., Christophe, M., & Defourny, P. (2013). National forest cover change in Congo Basin: deforestation, reforestation, degradation and regeneration for the years 1990, 2000 and 2005. *Global Change Biology*, *19*, 1173-1187.
- Esch, T., Metz, A., Marconcini, M., & Keil, M. (2014). Combined use of multi-seasonal high and medium resolution satellite imagery for parcel-related mapping of cropland and grassland. *International Journal of Applied Earth Observation and Geoinformation*, *28*, 230-237.
- Feng, Q., Liu, J., & Gong, J. (2015). UAV remote sensing for urban vegetation mapping using random forest and texture analysis. *Remote Sensing*, *7*, 1074-1094.
- Food and Agriculture Organization of the United Nations (2008). Terrestrial Essential Climate Variables for Climate Change Assessment, Mitigation and Adaptation; Global Terrestrial

- Observing System GTOS 52 – Biennial Report Supplement. In R. Sessa, & H. Dolman (Eds.). (Rome, Italy).
- Foody, G. M. (2002). Status of land cover classification accuracy assessment. *Remote Sensing of Environment*, 80, 185-201.
- Foody, G. M., & Mathur, A. (2004). A relative evaluation of multiclass image classification by support vector machines. *IEEE Transactions on Geoscience and Remote Sensing*, 42, 1335-1343.
- Forkuor, G., Hounkpatin, O. K., Welp, G., & Thiel, M. (2017). High Resolution Mapping of Soil Properties Using Remote Sensing Variables in South-Western Burkina Faso: A Comparison of Machine Learning and Multiple Linear Regression Models. *PloS One*, 12, e0170478.
- Franklin, S. E., & Wulder, M. A. (2002). Remote sensing methods in medium spatial resolution satellite data land cover classification of large areas. *Progress in Physical Geography*, 26, 173-205.
- Friedl, M. A., McIver, D. K., Hodges, J. C., Zhang, X. Y., Muchoney, D., Strahler, A. H., Woodcock, C.E., Gopal, S., Schneider, A., Cooper, A., Baccini, A., Gao, F., & Schaaf, C. (2002). Global land cover mapping from MODIS: algorithms and early results. *Remote Sensing of Environment*, 83, 287-302.
- Friedl, M. A., Sulla-Menashe, D., Tan, B., Schneider, A., Ramankutty, N., Sibley, A., & Huang, X. (2010). MODIS Collection 5 global land cover: Algorithm refinements and characterization of new datasets. *Remote sensing of Environment*, 114, 168-182.
- Fu, P., & Weng, Q. (2016). A time series analysis of urbanization induced land use and land cover change and its impact on land surface temperature with Landsat imagery. *Remote Sensing of Environment*, 175, 205-214.
- Genuer, R., Poggi, J. M., & Tuleau-Malot, C. (2010). Variable selection using random forests. *Pattern Recognition Letters*, 31, 2225-2236.
- Gessner, U., Knauer, K., Kuenzer, C., & Dech, S. (2015). Land surface phenology in a west african savanna: Impact of land use, land cover and fire. In *Remote Sensing Time Series* (pp. 203-223). Springer International Publishing.
- Ghimire, B., Rogan, J., & Miller, J. (2010). Contextual land-cover classification: incorporating spatial dependence in land-cover classification models using random forests and the Getis statistic. *Remote Sensing Letters*, 1, 45-54.
- Giglio, L. (2007). Characterization of the tropical diurnal fire cycle using VIRS and MODIS observations. *Remote Sensing of Environment*, 108, 407-421.
- Giglio, L., Randerson, J. T., Van der Werf, G. R., Kasibhatla, P. S., Collatz, G. J., Morton, D. C., & DeFries, R. S. (2010). Assessing variability and long-term trends in burned area by merging multiple satellite fire products. *Biogeosciences*, 7, 1171-1186.

- Gómez, C., White, J. C., & Wulder, M. A. (2016). Optical remotely sensed time series data for land cover classification: A review. *ISPRS Journal of Photogrammetry and Remote Sensing*, *116*, 55-72.
- Gonçalves, L. M., Fonte, C. C., Júlio, E. N., & Caetano, M. (2009). A method to incorporate uncertainty in the classification of remote sensing images. *International Journal of Remote Sensing*, *30*, 5489-5503.
- Gong, P., Wang, J., Yu, L., Zhao, Y., Zhao, Y., Liang, L., et al. (2013). Finer resolution observation and monitoring of global land cover: First mapping results with Landsat TM and ETM+ data. *International Journal of Remote Sensing*, *34*, 2607-2654.
- Goodwin, N. R., & Collett, L. J. (2014). Development of an automated method for mapping fire history captured in Landsat TM and ETM+ time series across Queensland, Australia. *Remote Sensing of Environment*, *148*, 206-221.
- Goodwin, N. R., Collett, L. J., Denham, R. J., Flood, N., & Tindall, D. (2013). Cloud and cloud shadow screening across Queensland, Australia: An automated method for Landsat TM/ETM+ time series. *Remote Sensing of Environment*, *134*, 50-65.
- Halperin, J., LeMay, V., Coops, N., Verchot, L., Marshall, P., & Lochhead, K. (2016). Canopy cover estimation in miombo woodlands of Zambia: comparison of Landsat 8 OLI versus RapidEye imagery using parametric, nonparametric, and semiparametric methods. *Remote Sensing of Environment*, *179*, 170-182.
- Hansen, M. C., DeFries, R. S., Townshend, J. R., & Sohlberg, R. (2000). Global land cover classification at 1 km spatial resolution using a classification tree approach. *International Journal of Remote Sensing*, *21*, 1331-1364.
- Hansen, M. C., DeFries, R. S., Townshend, J. R. G., Marufu, L., & Sohlberg, R. (2002). Development of a MODIS tree cover validation data set for Western Province, Zambia. *Remote Sensing of Environment*, *83*, 320-335.
- Haralick, R. M., Shanmugam, K., & Dinstein, I. (1973). Textural features for image classification. *IEEE Transactions on systems, man, and cybernetics*, *3*, 610-621.
- Hardtke, L. A., Blanco, P. D., del Valle, H. F., Metternicht, G. I., & Sione, W. F. (2015). Semi-automated mapping of burned areas in semi-arid ecosystems using MODIS time-series imagery. *International Journal of Applied Earth Observation and Geoinformation*, *38*, 25-35.
- Heiskanen, J. (2006). Tree cover and height estimation in the Fennoscandian tundra-taiga transition zone using multiangular MISR data. *Remote Sensing of Environment*, *103*, 97-114.
- Heiskanen, J., & Kivinen, S. (2008). Assessment of multispectral,-temporal and-angular MODIS data for tree cover mapping in the tundra-taiga transition zone. *Remote Sensing of Environment*, *112*, 2367-2380.
- Herold, M., Latham, J. S., Di Gregorio, A., & Schmullius, C. C. (2006). Evolving standards in land cover characterization. *Journal of Land Use Science*, *1*, 157-168.

- Herold, M., See, L., Tsensbazar, N. E., & Fritz, S. (2016). Towards an Integrated Global Land Cover Monitoring and Mapping System. *Remote Sensing*, 8, 1036.
- Herold, M., Woodcock, C. E., Loveland, T. R., Townshend, J., Brady, M., Steenmans, C., & Schullius, C. C. (2008). Land-cover observations as part of a Global Earth Observation System of Systems (GEOSS): Progress, Activities, and prospects. *IEEE Systems Journal*, 2, 414-423.
- Higgins, S. I., Bond, W. J., & Trollope, W. S. (2000). Fire, resprouting and variability: a recipe for grass–tree coexistence in savanna. *Journal of Ecology*, 88, 213-229.
- Hijmans, R. J., Cameron, S. E., Parra, J. L., Jones, P. G., & Jarvis, A. (2005). Very high resolution interpolated climate surfaces for global land areas. *International Journal of Climatology*, 25, 1965-1978.
- Huang, C., Goward, S. N., Schleeuwis, K., Thomas, N., Masek, J. G., & Zhu, Z. (2009). Dynamics of national forests assessed using the Landsat record: Case studies in eastern United States. *Remote sensing of Environment*, 113, 1430-1442.
- Huang, X., Zhang, L., & Li, P. (2007). An adaptive multiscale information fusion approach for feature extraction and classification of IKONOS multispectral imagery over urban areas. *IEEE Geoscience and Remote Sensing Letters*, 4, 654-658.
- Ibrahim, M. A., Arora, M. K., & Ghosh, S. K. (2005). Estimating and accommodating uncertainty through the soft classification of remote sensing data. *International Journal of Remote Sensing*, 26, 2995-3007.
- Jakubauskas, M. E., Legates, D. R., & Kastens, J. H. (2002). Crop identification using harmonic analysis of time-series AVHRR NDVI data. *Computers and Electronics in Agriculture*, 37, 127-139.
- Jia, K., Liang, S., Zhang, N., Wei, X., Gu, X., Zhao, X., Yao, Y., & Xie, X. (2014). Land cover classification of finer resolution remote sensing data integrating temporal features from time series coarser resolution data. *ISPRS Journal of Photogrammetry and Remote Sensing*, 93, 49-55.
- Jönsson, P., & Eklundh, L. (2004). TIMESAT—a program for analyzing time-series of satellite sensor data. *Computers & Geosciences*, 30, 833-845.
- Joshi, N., Baumann, M., Ehammer, A., Fensholt, R., Grogan, K., Hostert, P., et al. (2016). A review of the application of optical and radar remote sensing data fusion to land use mapping and monitoring. *Remote Sensing*, 8, 70.
- Jung, M., Henkel, K., Herold, M., & Churkina, G. (2006). Exploiting synergies of global land cover products for carbon cycle modeling. *Remote Sensing of Environment*, 101, 534-553.
- Justice, C. O., Townshend, J. R. G., Vermote, E. F., Masuoka, E., Wolfe, R. E., Saleous, N., Roy, D.P., & Morisette, J. T. (2002). An overview of MODIS Land data processing and product status. *Remote sensing of Environment*, 83, 3-15.

- Kalema, V. N., Witkowski, E. T., Erasmus, B. F., & Mwavu, E. N. (2015). The impacts of changes in land use on woodlands in an equatorial African savanna. *Land Degradation & Development*, *26*, 632-641.
- Karlson, M., Ostwald, M., Reese, H., Sanou, J., Tankoano, B., & Mattsson, E. (2015). Mapping tree canopy cover and aboveground biomass in Sudano-Sahelian woodlands using Landsat 8 and random forest. *Remote Sensing*, *7*, 10017-10041.
- Kayitakire, F., Hamel, C., & Defourny, P. (2006). Retrieving forest structure variables based on image texture analysis and IKONOS-2 imagery. *Remote Sensing of Environment*, *102*, 390-401.
- Kelsey, K. C., & Neff, J. C. (2014). Estimates of aboveground biomass from texture analysis of Landsat imagery. *Remote Sensing*, *6*, 6407-6422.
- Kennedy, R. E., Cohen, W. B., & Schroeder, T. A. (2007). Trajectory-based change detection for automated characterization of forest disturbance dynamics. *Remote Sensing of Environment*, *110*, 370-386.
- Knauer, K., Gessner, U., Fensholt, R., Forkuor, G., & Kuenzer, C. (2017). Monitoring agricultural expansion in burkina faso over 14 years with 30 m resolution time series: the role of population growth and implications for the environment. *Remote Sensing*, *9*, 132.
- Kontoes, C. C., Poilvé, H., Florsch, G., Keramitsoglou, I., & Paralikidis, S. (2009). A comparative analysis of a fixed thresholding vs. a classification tree approach for operational burn scar detection and mapping. *International Journal of Applied Earth Observation and Geoinformation*, *11*, 299-316.
- Koutsias, N., Mallinis, G., & Karteris, M. (2009). A forward/backward principal component analysis of Landsat-7 ETM+ data to enhance the spectral signal of burnt surfaces. *ISPRS Journal of Photogrammetry and Remote Sensing*, *64*, 37-46.
- Koutsias, N., & Pleniou, M. (2015). Comparing the spectral signal of burned surfaces between Landsat 7 ETM+ and Landsat 8 OLI sensors. *International Journal of Remote Sensing*, *36*, 3714-3732.
- Koutsias, N., Pleniou, M., Mallinis, G., Nioti, F., & Sifakis, N. I. (2013). A rule-based semi-automatic method to map burned areas: exploring the USGS historical Landsat archives to reconstruct recent fire history. *International Journal of Remote Sensing*, *34*, 7049-7068.
- Lambin, E. F., Turner, B. L., Geist, H. J., Agbola, S. B., Angelsen, A., Bruce, J. W., Coomes, O. T., Dirzo, R., Fischer, G., Folke, C., George, P. S., & George, P. (2001). The causes of land-use and land-cover change: moving beyond the myths. *Global Environmental Change*, *11*, 261-269.
- Laris, P. S. (2005). Spatiotemporal problems with detecting and mapping mosaic fire regimes with coarse-resolution satellite data in savanna environments. *Remote Sensing of Environment*, *99*, 412-424.

- Liu, J., Heiskanen, J., Aynekulu, E., & Pellikka, P. K. E. (2015). Seasonal variation of land cover classification accuracy of Landsat 8 images in Burkina Faso. *The International Archives of Photogrammetry, Remote Sensing and Spatial Information Sciences*, 40, 455.
- Liu, H., & Zhou, Q. (2005). Developing urban growth predictions from spatial indicators based on multi-temporal images. *Computers, Environment and Urban Systems*, 29, 580-594.
- Loveland, T. R., Reed, B. C., Brown, J. F., Ohlen, D. O., Zhu, Z., Yang, L. W. M. J., & Merchant, J. W. (2000). Development of a global land cover characteristics database and IGBP DISCover from 1 km AVHRR data. *International Journal of Remote Sensing*, 21, 1303-1330.
- Maeda, E. E., Formaggio, A. R., Shimabukuro, Y. E., Arcoverde, G. F. B., & Hansen, M. C. (2009). Predicting forest fire in the Brazilian Amazon using MODIS imagery and artificial neural networks. *International Journal of Applied Earth Observation and Geoinformation*, 11, 265-272.
- Maeda, E. E., Heiskanen, J., Thijs, K. W., & Pellikka, P. K. (2014). Season-dependence of remote sensing indicators of tree species diversity. *Remote Sensing Letters*, 5, 404-412.
- Miller, S. N., Phillip Guertin, D., & Goodrich, D. C. (2007). Hydrologic Modeling Uncertainty Resulting From Land Cover Misclassification. *Journal of the American Water Resources Association*, 43, 1065-1075.
- Miller, J. D., & Thode, A. E. (2007). Quantifying burn severity in a heterogeneous landscape with a relative version of the delta Normalized Burn Ratio (dNBR). *Remote Sensing of Environment*, 109, 66-80.
- Mitchard, E. T. A., Saatchi, S. S., White, L. J. T., Abernethy, K. A., Jeffery, K. J., Lewis, S. L., Collins, M., Leal, M. E., Woodhouse, I. H., & Meir, P. (2011). Mapping tropical forest biomass with radar and spaceborne LiDAR: overcoming problems of high biomass and persistent cloud. *Biogeosciences Discussions*, 8, 8781.
- Mouillot, F., Schultz, M. G., Yue, C., Cadule, P., Tansey, K., Ciais, P., & Chuvieco, E. (2014). Ten years of global burned area products from spaceborne remote sensing—A review: Analysis of user needs and recommendations for future developments. *International Journal of Applied Earth Observation and Geoinformation*, 26, 64-79.
- Mountrakis, G., Im, J., & Ogole, C. (2011). Support vector machines in remote sensing: A review. *ISPRS Journal of Photogrammetry and Remote Sensing*, 66, 247-259.
- Müller, H., Rufin, P., Griffiths, P., Siqueira, A. J. B., & Hostert, P. (2015). Mining dense Landsat time series for separating cropland and pasture in a heterogeneous Brazilian savanna landscape. *Remote Sensing of Environment*, 156, 490-499.
- Musyimi, Z., Said, M. Y., Zida, D., Rosenstock, T. S., Udelhoven, T., Savadogo, P., Leeuw, J. d., & Aynekulu, E. (2017). Evaluating fire severity in Sudanian ecosystems of Burkina Faso using Landsat 8 satellite images. *Journal of Arid Environments*, 139, 95-109.
- Myint, S. W., Lam, N. S. N., & Tyler, J. M. (2004). Wavelets for urban spatial feature discrimination. *Photogrammetric Engineering & Remote Sensing*, 70, 803-812.

- Nielsen, T. T., & Rasmussen, K. (1997). The distribution in time and space of savanna fires in Burkina Faso as determined from NOAA AVHRR data. *Geografisk Tidsskrift-Danish Journal of Geography*, *97*, 86-97.
- Oldeland, J., Wesuls, D., Rocchini, D., Schmidt, M., & Jürgens, N. (2010). Does using species abundance data improve estimates of species diversity from remotely sensed spectral heterogeneity? *Ecological Indicators*, *10*, 390-396.
- Olson, D. M., Dinerstein, E., Wikramanayake, E. D., Burgess, N. D., Powell, G. V., Underwood, E. C., et al. (2001). Terrestrial Ecoregions of the World: A New Map of Life on Earth: A new global map of terrestrial ecoregions provides an innovative tool for conserving biodiversity. *BioScience*, *51*, 933-938.
- Ouedraogo, I., Savadogo, P., Tigabu, M., Cole, R., Odén, P. C., & Ouadba, J. M. (2009). Is rural migration a threat to environmental sustainability in Southern Burkina Faso? *Land Degradation & Development*, *20*, 217-230.
- Ouma, Y. O., Ngigi, T. G., & Tateishi, R. (2006). On the optimization and selection of wavelet texture for feature extraction from high-resolution satellite imagery with application towards urban-tree delineation. *International Journal of Remote Sensing*, *27*, 73-104.
- Pacifici, F., Chini, M., & Emery, W. J. (2009). A neural network approach using multi-scale textural metrics from very high-resolution panchromatic imagery for urban land-use classification. *Remote Sensing of Environment*, *113*, 1276-1292.
- Pal, M., & Mather, P. M. (2005). Support vector machines for classification in remote sensing. *International Journal of Remote Sensing*, *26*, 1007-1011.
- Pargal, S., Fararoda, R., Rajashekar, G., Balachandran, N., Réjou-Méchain, M., Barbier, N., Jha, C. S., Péliissier, R., Dadhwal, V. K., & Couteron, P. (2017). Inverting Aboveground Biomass–Canopy Texture Relationships in a Landscape of Forest Mosaic in the Western Ghats of India Using Very High Resolution Cartosat Imagery. *Remote Sensing*, *9*, 228.
- Pellikka, P., Seed, E. D., & King, D. J. (2000). Modelling deciduous forest ice storm damage using aerial CIR imagery and hemispheric photography. *Canadian Journal of Remote Sensing*, *26*, 394-405.
- Pengra, B., Long, J., Dahal, D., Stehman, S. V., & Loveland, T. R. (2015). A global reference database from very high resolution commercial satellite data and methodology for application to Landsat derived 30m continuous field tree cover data. *Remote Sensing of Environment*, *165*, 234-248.
- Pesaresi, M. (2000). Texture analysis for urban pattern recognition using fine-resolution panchromatic satellite imagery. *Geographical and Environmental Modelling*, *4*, 43-63.
- Potapov, P. V., Turubanova, S. A., Hansen, M. C., Adusei, B., Broich, M., Altstatt, A., Mane, L., & Justice, C. O. (2012). Quantifying forest cover loss in Democratic Republic of the Congo, 2000–2010, with Landsat ETM+ data. *Remote Sensing of Environment*, *122*, 106-116.

- Puissant, A., Hirsch, J., & Weber, C. (2005). The utility of texture analysis to improve per-pixel classification for high to very high spatial resolution imagery. *International Journal of Remote Sensing*, 26, 733-745.
- Rocchini, D., Boyd, D. S., Féret, J. B., Foody, G. M., He, K. S., Lausch, A., Nagendra, H., Wegmann, M., & Pettorelli, N. (2015). Satellite remote sensing to monitor species diversity: potential and pitfalls. *Remote Sensing in Ecology and Conservation*, 2, 25-36.
- Roy, D. P., & Boschetti, L. (2009). Southern Africa validation of the MODIS, L3JRC, and GlobCarbon burned-area products. *IEEE transactions on Geoscience and Remote Sensing*, 47, 1032-1044.
- Roy, D. P., Boschetti, L., Justice, C. O., & Ju, J. (2008). The collection 5 MODIS burned area product—Global evaluation by comparison with the MODIS active fire product. *Remote Sensing of Environment*, 112, 3690-3707.
- Sarker, L. R., & Nichol, J. E. (2011). Improved forest biomass estimates using ALOS AVNIR-2 texture indices. *Remote Sensing of Environment*, 115, 968-977.
- Sawadogo, L., Nygård, R., & Pallo, F. (2002). Effects of livestock and prescribed fire on coppice growth after selective cutting of Sudanian savannah in Burkina Faso. *Annals of Forest Science*, 59, 185-195.
- Schroeder, W., Prins, E., Giglio, L., Csiszar, I., Schmidt, C., Morisette, J., & Morton, D. (2008). Validation of GOES and MODIS active fire detection products using ASTER and ETM+ data. *Remote Sensing of Environment*, 112, 2711-2726.
- Senf, C., Leitão, P. J., Pflugmacher, D., van der Linden, S., & Hostert, P. (2015). Mapping land cover in complex Mediterranean landscapes using Landsat: Improved classification accuracies from integrating multi-seasonal and synthetic imagery. *Remote Sensing of Environment*, 156, 527-536.
- Shaban, M. A., & Dikshit, O. (2001). Improvement of classification in urban areas by the use of textural features: the case study of Lucknow city, Uttar Pradesh. *International Journal of Remote Sensing*, 22, 565-593.
- Siljander, M. (2009). Predictive fire occurrence modelling to improve burned area estimation at a regional scale: a case study in East Caprivi, Namibia. *International Journal of Applied Earth Observation and Geoinformation*, 11, 380-393.
- Silva, J. M., Sá, A. C., & Pereira, J. M. (2005). Comparison of burned area estimates derived from SPOT-VEGETATION and Landsat ETM+ data in Africa: Influence of spatial pattern and vegetation type. *Remote sensing of environment*, 96, 188-201.
- Song, C., Woodcock, C. E., Seto, K. C., Lenney, M. P., & Macomber, S. A. (2001). Classification and change detection using Landsat TM data: When and how to correct atmospheric effects? *Remote sensing of Environment*, 75, 230-244.
- St-Louis, V., Pidgeon, A. M., Radeloff, V. C., Hawbaker, T. J., & Clayton, M. K. (2006). High-resolution image texture as a predictor of bird species richness. *Remote Sensing of Environment*, 105, 299-312.

- Stroppiana, D., Bordogna, G., Carrara, P., Boschetti, M., Boschetti, L., & Brivio, P. A. (2012). A method for extracting burned areas from Landsat TM/ETM+ images by soft aggregation of multiple Spectral Indices and a region growing algorithm. *ISPRS Journal of Photogrammetry and Remote Sensing*, *69*, 88-102.
- Tansey, K., Grégoire, J. M., Defourny, P., Leigh, R., Pekel, J. F., van Bogaert, E., & Bartholomé, E. (2008). A new, global, multi-annual (2000–2007) burnt area product at 1 km resolution. *Geophysical Research Letters*, *35*, L01401.
- Torello-Raventos, M., Feldpausch, T. R., Veenendaal, E., Schrodte, F., Saiz, G., Domingues, T. F., et al. (2013). On the delineation of tropical vegetation types with an emphasis on forest/savanna transitions. *Plant Ecology & Diversity*, *6*, 101-137.
- Townshend, J. R., & Justice, C. O. (1988). Selecting the spatial resolution of satellite sensors required for global monitoring of land transformations. *International Journal of Remote Sensing*, *9*, 187-236.
- Vågen, T.-G., Winowiecki, L., Desta, L. T., & Tondoh, J. E. (2013). The land degradation surveillance framework (LDSF) - field guide v3-2013. *Nairobi: World Agroforestry Centre (ICRAF)*.
- Valbuena, R., Heiskanen, J., Aynekulu, E., Pitkänen, S., & Packalen, P. (2016). Sensitivity of Above-Ground Biomass Estimates to Height-Diameter Modelling in Mixed-Species West African Woodlands. *PLoS One*, *11*, e0158198.
- Verbesselt, J., Zeileis, A., & Herold, M. (2012). Near real-time disturbance detection using satellite image time series. *Remote Sensing of Environment*, *123*, 98-108.
- Vivchar, A. (2011). Wildfires in Russia in 2000–2008: estimates of burnt areas using the satellite MODIS MCD45 data. *Remote Sensing Letters*, *2*, 81-90.
- Wang, L., & Zhang, S. (2014). Incorporation of texture information in a SVM method for classifying salt cedar in western China. *Remote Sensing Letters*, *5*, 501-510.
- White, J. C., Wulder, M. A., Hobart, G. W., Luther, J. E., Hermosilla, T., Griffiths, P., Coops, N. C., Hall, R. J., Hostert, P., Dyk, A., & Guindon, L. (2014). Pixel-based image compositing for large-area dense time series applications and science. *Canadian Journal of Remote Sensing*, *40*, 192-212.
- Woodcock, C. E., Allen, A. A., Anderson, M., Belward, A. S., Bindschadler, R., Cohen, W. B., Gao, F., Goward, S. N., Helder, D., Helmer, E., Nemani, R., Oreopoulos, L., Schott, J., Thenkabail, P. S., Vermote, E. F., Vogelmann, J., Wulder, M. A., & Wynne, R. (2008). Free access to Landsat imagery. *Science*, *320*, 1011.
- Wu, C., Hou, X., Peng, D., Gonsamo, A., & Xu, S. (2016). Land surface phenology of China's temperate ecosystems over 1999–2013: Spatial-temporal patterns, interaction effects, covariation with climate and implications for productivity. *Agricultural and Forest Meteorology*, *216*, 177-187.
- Wulder, M. A., & Coops, N. C. (2014). Make Earth observations open access. *Nature*, *513*, 30.

- Wulder, M. A., Hilker, T., White, J. C., Coops, N. C., Masek, J. G., Pflugmacher, D., & Crevier, Y. (2015). Virtual constellations for global terrestrial monitoring. *Remote Sensing of Environment*, 170, 62-76.
- Wulder, M. A., Masek, J. G., Cohen, W. B., Loveland, T. R., & Woodcock, C. E. (2012). Opening the archive: How free data has enabled the science and monitoring promise of Landsat. *Remote Sensing of Environment*, 122, 2-10.
- Xiao, X., Boles, S., Liu, J., Zhuang, D., & Liu, M. (2002). Characterization of forest types in Northeastern China, using multi-temporal SPOT-4 VEGETATION sensor data. *Remote Sensing of Environment*, 82, 335-348.
- Xue, X., Liu, H., Mu, X., & Liu, J. (2014). Trajectory-based detection of urban expansion using Landsat time series. *International Journal of Remote Sensing*, 35, 1450-1465.
- Zhu, X., & Liu, D. (2015). Improving forest aboveground biomass estimation using seasonal Landsat NDVI time-series. *ISPRS Journal of Photogrammetry and Remote Sensing*, 102, 222-231.
- Zhu, Z., Woodcock, C. E., Rogan, J., & Kelldorfer, J. (2012a). Assessment of spectral, polarimetric, temporal, and spatial dimensions for urban and peri-urban land cover classification using Landsat and SAR data. *Remote Sensing of Environment*, 117, 72-82.
- Zhu, Z., & Woodcock, C. E. (2012b). Object-based cloud and cloud shadow detection in Landsat imagery. *Remote Sensing of Environment*, 118, 83-94.
- Zhu, Z., Woodcock, C. E., & Olofsson, P. (2012c). Continuous monitoring of forest disturbance using all available Landsat imagery. *Remote Sensing of Environment*, 122, 75-91.
- Zhu, Z., & Woodcock, C. E. (2014a). Continuous change detection and classification of land cover using all available Landsat data. *Remote sensing of Environment*, 144, 152-171.
- Zhu, Z., & Woodcock, C. E. (2014b). Automated cloud, cloud shadow, and snow detection in multitemporal Landsat data: An algorithm designed specifically for monitoring land cover change. *Remote Sensing of Environment*, 152, 217-234.